iScience

CellPress

Article

Transcriptional Co-activator Functions of YAP and TAZ Are Inversely Regulated by Tyrosine Phosphorylation Status of Parafibromin

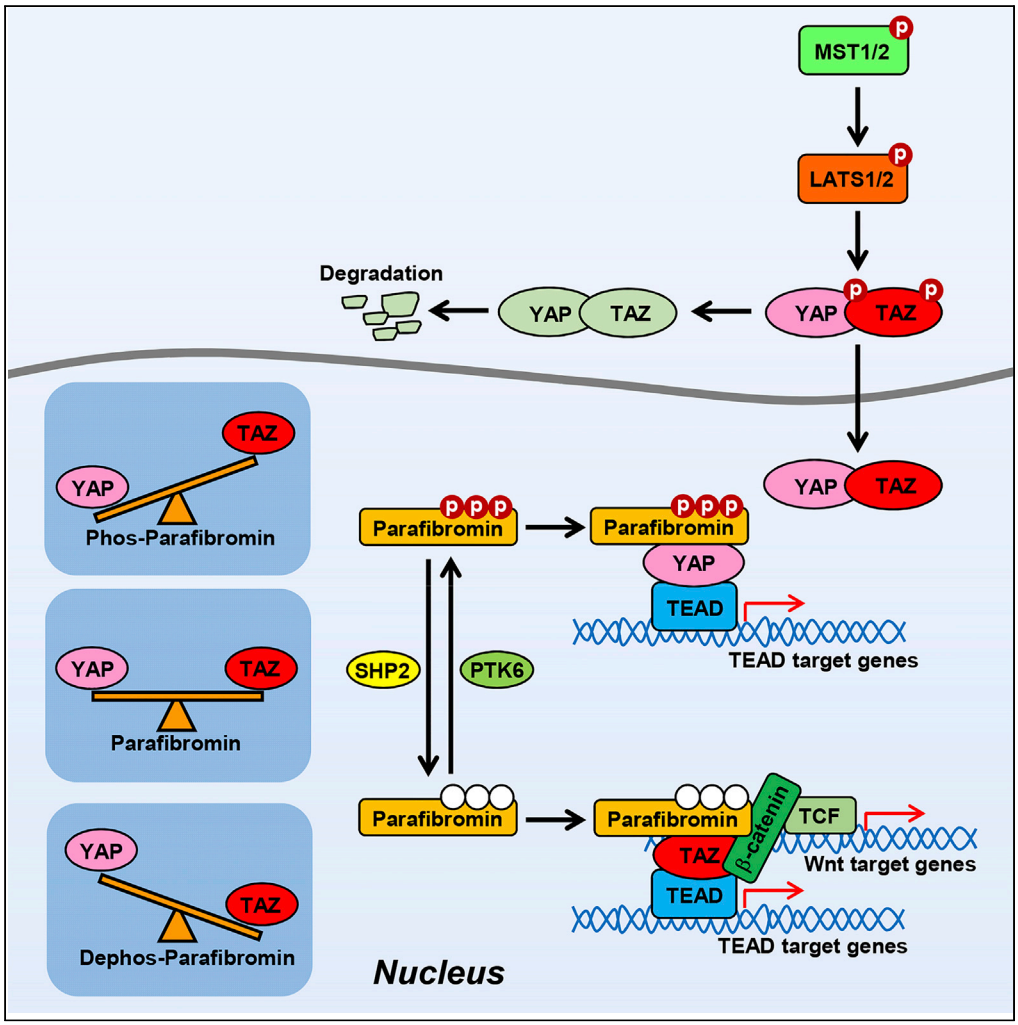

Chao Tang, Atsushi Takahashi-Kanemitsu, Ippei Kikuchi, Chi Ben, Masanori Hatakeyama

mhata@m.u-tokyo.ac.jp

HIGHLIGHTS

YAP and TAZ co-activators bind to the nuclear tyrosine phosphoprotein Parafibromin

TAZ is functionally activated through binding with dephosphorylated Parafibromin

YAP activity is stimulated upon binding with tyrosine-phosphorylated Parafibromin

Dephosphorylated Parafibromin co-stimulates TAZ and β-catenin via complex formation

Tang et al., iScience 1, 1–15 March 23, 2018
https://doi.org/10.1016/j.isci.2018.01.003

iScience

CellPress

Article

Transcriptional Co-activator Functions of YAP and TAZ Are Inversely Regulated by Tyrosine Phosphorylation Status of Parafibromin

Chao Tang,[1] Atsushi Takahashi-Kanemitsu,[1] Ippei Kikuchi,[1] Chi Ben,[1] and Masanori Hatakeyama[1,2,*]

SUMMARY

YAP and TAZ, the Hippo signal-regulated transcriptional co-activators, play crucial roles in morphogenesis and organogenesis. Here we report that the YAP/TAZ activities are stimulated upon complex formation with Parafibromin, which undergoes tyrosine phosphorylation and dephosphorylation by kinases such as PTK6 and phosphatases such as SHP2, respectively. Furthermore, TAZ and the Wnt effector β-catenin interact cooperatively with tyrosine-dephosphorylated Parafibromin, which synergistically stimulates the co-activator functions of TAZ and β-catenin. On the other hand, YAP is selectively activated through binding with tyrosine-phosphorylated Parafibromin, which does not interact with β-catenin and thus cannot co-activate YAP and β-catenin. These findings indicate that Parafibromin inversely regulates the activities of YAP and TAZ depending on its tyrosine phosphorylation status. They also suggest that YAP and TAZ exert their redundant and non-redundant biological actions through mutually exclusive interaction with Parafibromin, which is regulated by a balance of kinase and phosphatase activities toward Parafibromin.

INTRODUCTION

The Hippo signaling pathway, which was first identified in *Drosophila,* plays a key role in organ size determination and tissue homeostasis (Pan, 2010; Yu et al., 2015; Pfleger, 2017). A unique feature of the Hippo signal is that it mediates contact inhibition of cell growth/proliferation by sensing cell density through mechanisms yet to be fully understood (Zhao et al., 2007; Gumbiner and Kim, 2014). The core components and downstream effectors of the Hippo pathway are highly conserved from *Drosophila* to mammals. In mammals, when Hippo signaling is activated, pro-apoptotic kinases MST1/2, complexed with the scaffold protein WW45/SAV1, phosphorylate and activate LATS1/2 kinases, which in turn phosphorylate the transcription co-activator Yes-associated protein (YAP) and the transcriptional co-activator with PDZ-binding motif (TAZ, also called WWTR1) (Guo and Teng, 2015; Hansen et al., 2015). TAZ is the one and only paralog of YAP, sharing 46% overall amino acid sequence identity with very similar structural topology (Wang et al., 2009). The E3 ubiquitin ligase $SCF^{\beta\text{-}TRCP}$ is then recruited to the phosphorylated YAP/TAZ, leading to their polyubiquitination and degradation in the cytoplasm (Zhao et al., 2010). Activation of membrane receptors such as G-protein-coupled receptors (GPCRs) and epidermal growth factor (EGF) receptor inhibits the Hippo signal and thereby allows nuclear translocalization and accumulation of YAP/TAZ (Yu et al., 2012; Fan et al., 2013). In the nucleus, YAP/TAZ interact with numerous transcription factors. Of these, the TEAD domain family proteins (TEADs), comprising four members (TEAD1–4), are major YAP/TAZ targets that play central roles in YAP/TAZ-mediated activation of genes involved in a diverse array of biological actions, including cell proliferation, cell survival, migration, cell invasion, epithelial-to-mesenchymal transition (EMT), stem cell renewal, and tumorigenesis (Pobbati and Hong, 2013; Zhou et al., 2016). Thus, YAP and TAZ share redundant functions by acting as transcriptional co-activators toward TEADs. In turn, the growth inhibitory action of Hippo signaling circumvents accumulation of YAP/TAZ in the nucleus, where they act as transcriptional co-activators. Pro-oncogenic actions of YAP/TAZ, such as elevated cell migration/invasion, EMT, and anchorage-independent colony formation, are due primarily to elevated TEAD-dependent transcription. Apart from these overlapping functions, YAP and TAZ also exhibit unique/non-redundant functions in a cell-type- and tissue-context-dependent manner. In fact, knockout of the *Yap* gene in mice is embryonically lethal (Morin-Kensicki et al., 2006). In contrast, *Taz* knockout does not perturb fetal development or fertility in mice, although it impairs the development and function of the lung and kidney (Hossain et al., 2007; Makita et al., 2008). These knockout phenotypes provide genetic evidence for the different biological roles of YAP

[1]Division of Microbiology, Graduate School of Medicine, The University of Tokyo, Tokyo 113-0033, Japan

[2]Lead Contact

*Correspondence: mhata@m.u-tokyo.ac.jp

https://doi.org/10.1016/j.isci.2018.01.003

and TAZ. Although interaction with different transcription factors may explain their differential actions, the mechanisms underpinning the unique biological functions of YAP and TAZ remain unknown.

Parafibromin, a predominantly nuclear protein encoded by the *HRPT2* (*hyperparathyroidism-jaw tumor type 2*) gene, is a mammalian ortholog of budding yeast Cdc73, a component of the PAF (RNA polymerase II associated factor) complex that plays a pleiotropic role in both transcriptional and post-transcriptional regulations of gene expression (Rozenblatt-Rosen et al., 2005; Yart et al., 2005; Chaudhary et al., 2007). Loss-of-function mutations in *HRPT2* have been shown to be associated with both familial and sporadic forms of parathyroid cancer, indicating its tumor suppressive role in the parathyroid gland (Carpten et al., 2002; Wang et al., 2005). Parafibromin is also involved in the regulation of morphogenesis and homeostasis in metazoans by acting as a nuclear scaffold that interacts with transcriptional co-activators/transcription factors for morphogen signaling pathways, such as Wnt-regulated β-catenin, Hedgehog-regulated Gli1, and Notch-regulated NICD (Notch intracellular domain), and thereby coordinates activation of genes targeted by these morphogens (Mosimann et al., 2006, 2009; Takahashi et al., 2011; Kikuchi et al., 2016). We previously reported that physical interaction of YAP/TAZ with the protein tyrosine phosphatase SHP2 is required for translocalization of SHP2 from the cytoplasm to the nucleus (Tsutsumi et al., 2013), in which SHP2 undergoes tyrosine dephosphorylation of Parafibromin on Tyr-290, Tyr-293, and Tyr-315. Dephosphorylated Parafibromin binds to β-catenin and Gli1 in a mutually exclusive manner to selectively activate the Wnt- and Hedgehog-dependent genes, respectively (Kikuchi et al., 2016).

In this study, we found that Parafibromin physically interacts with YAP and TAZ and thereby potentiates their co-activator activities toward the TEAD transcription factors. Like the cases of previously reported co-activators such as β-catenin and Gli1, Parafibromin-TAZ interaction and subsequent potentiation of TAZ-dependent TEAD activation required Parafibromin tyrosine dephosphorylation. On the other hand, Parafibromin-YAP interaction was independent of the tyrosine phosphorylation status of Parafibromin and, in direct opposition to TAZ, the co-activator function of YAP on TEAD was specifically potentiated by tyrosine-phosphorylated Parafibromin. The present work thus showed that Parafibromin is a context-dependent scaffold for YAP and TAZ, which contributes to both redundant and non-redundant functions of YAP/TAZ.

RESULTS

Stimulation of Co-activator Functions of YAP/TAZ by Parafibromin

To investigate the functional relationship between YAP/TAZ and Parafibromin, we conducted a reporter assay by ectopically expressing a Parafibromin vector and the 8xGT TEAD luciferase reporter plasmid in HEK293T human embryonic kidney cells and found that Parafibromin stimulates the TEAD reporter activity (Figure 1A). Similarly, elevated Parafibromin increased the levels of mRNAs for *Cyr61* and *Ctgf*, two *bona fide* TEAD target genes, in HEK293T cells (Hsu et al., 2015; Shimomura et al., 2014) (Figure 1B). In humans, YAP comprises two major splicing isoforms, YAP1 and YAP2, each of which is further subclassified into four different splicing variants (α, β, γ, δ). Among those, YAP1 isoforms (YAP1α, YAP1β, YAP1γ, and YAP1δ) contain a single WW domain, whereas YAP2 isoforms (YAP2α, YAP2β, YAP2γ, and YAP2δ) contain two WW domains (Hoshino et al., 2006; Webb et al., 2011). In contrast to YAP, TAZ does not exhibit distinctive splicing variations and possesses only one WW domain. To substantiate YAP/TAZ-dependent TEAD activation, we performed a TEAD luciferase reporter assay in HEK293T cells transiently co-expressing Parafibromin and YAP or TAZ. To do so, we used two YAP isoforms, YAP1α and YAP2δ, the shortest and the longest splicing isoforms, respectively. The results of the experiment revealed that single expression of YAP1α, YAP2δ, or TAZ stimulated TEAD reporter activity and that co-expression of Parafibromin further potentiated the reporter activation (Figures 1C and 1D). These results were reproduced in HEK293A cells, which do not express the SV40 large T antigen, and in AGS human gastric epithelial cells (Figures S1A–S1D). Notably, the magnitude of TEAD reporter activation was substantially greater in cells co-expressing Parafibromin and YAP2δ than in cells co-expressing Parafibromin and YAP1α, suggesting that YAP isoforms containing two WW domains stimulate TEAD-dependent transcription more strongly than do YAP isoforms containing a single WW domain (Figure 1C). Next, to examine the involvement of endogenous Parafibromin in the co-activator functions of YAP/TAZ, we knocked out the *HRPT2* gene, which encodes Parafibromin, in HEK293T cells by transfecting an expression vector for the *HRPT2*-specific single guide (sg) RNA. The results of the reporter assay revealed that the inhibition of Parafibromin expression not only diminished the basal TEAD reporter activity, which was rescued by ectopic expression of Parafibromin, but also impaired TEAD reporter activation by ectopic YAP2δ or TAZ expression (Figures 1E, S1E, and S1F). *HRPT2* knockout in HEK293T cells was also associated with reduced levels of *Cyr61* and *Ctgf* mRNAs

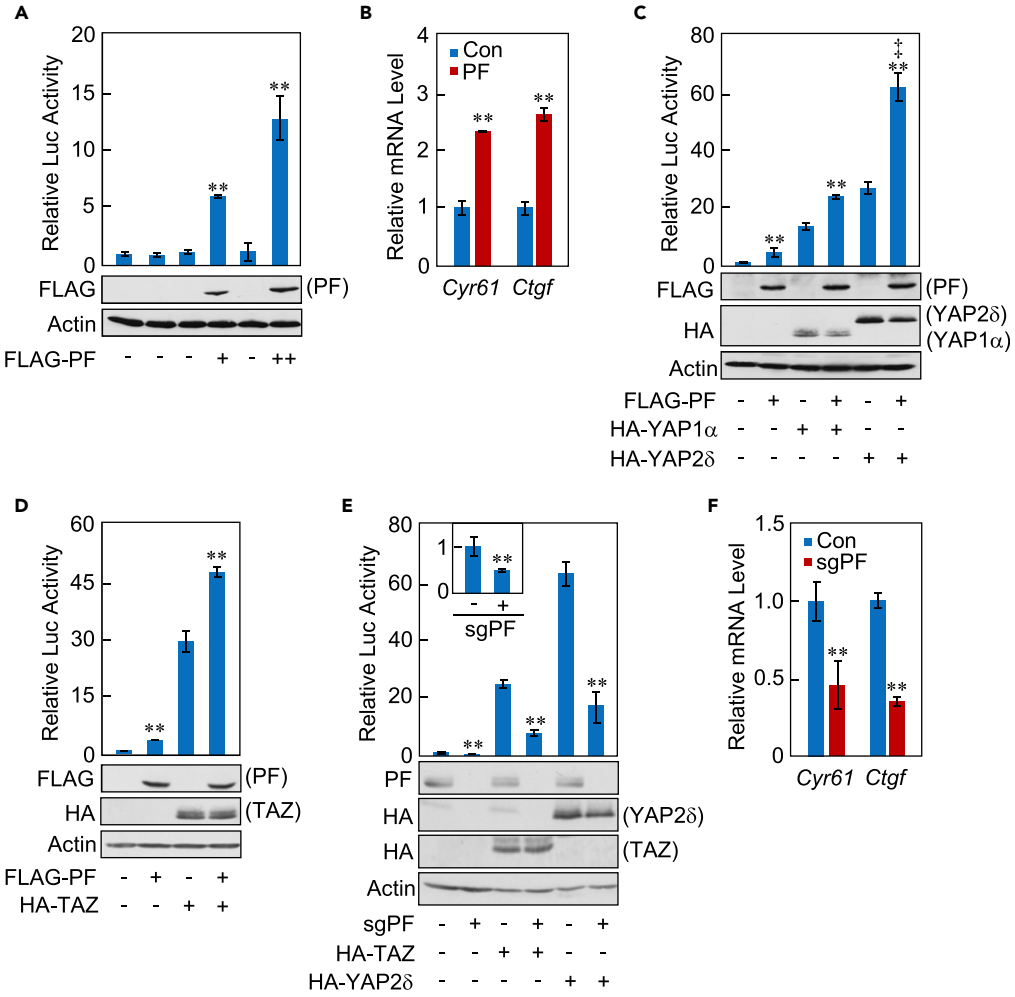

Figure 1. Potentiation of the Transcriptional Co-activator Activity of YAP and TAZ toward TEAD by Parafibromin

(A) HEK293T cells were transiently transfected with a TEAD luciferase reporter together with the indicated plasmids. Total cell lysates were subjected to luciferase assay and immunoblotting with indicated antibodies. PF, Parafibromin.

(B) Quantitative reverse transcription polymerase chain reaction (qRT-PCR) analysis of *Cyr61* and *Ctgf* mRNA expression in HEK293T cells transiently transfected with a PF or control empty vector (Con).

(C and D) HEK293T cells were transiently transfected with a TEAD luciferase reporter together with indicated plasmids. Total cell lysates were subjected to luciferase assay and immunoblotting with indicated antibodies.

(E) HEK293T cells were transiently transfected with indicated plasmids. Total cell lysates were subjected to luciferase assay and immunoblotting with indicated antibodies.

(F) qRT-PCR analysis of *Cyr61* and *Ctgf* mRNA expression in HEK293T cells transiently transfected with sgPF vector or a control vector.

Error bars, mean ± SD; n = 3; **p < 0.01 versus control vector (A–F), YAP1α with control vector (C), YAP2δ with control vector (C and E), or TAZ with control vector (D and E); ‡p < 0.01 versus YAP1α with PF (C).

See also Figure S1.

(Figure 1F). Collectively, these observations indicated that Parafibromin potentiates the co-activator function of YAP/TAZ toward TEAD transcription factors.

Enhancement of YAP/TAZ-Mediated Biological Actions by Parafibromin

The biological importance of the functional interaction between Parafibromin and YAP/TAZ was next investigated by a wound healing assay, which evaluates the magnitude of YAP/TAZ-mediated TEAD activation (Zhang et al., 2009a, 2009b). Expression of a gain-of-function mutant of TAZ, TAZ^{S89A}, in AGS cells accelerated gap closure. The effect of TAZ^{S89A} was, however, abolished by specific knockout of Parafibromin in the cells (Figure 2A). YAP and TAZ have also been reported to stimulate cell growth via TEAD activation

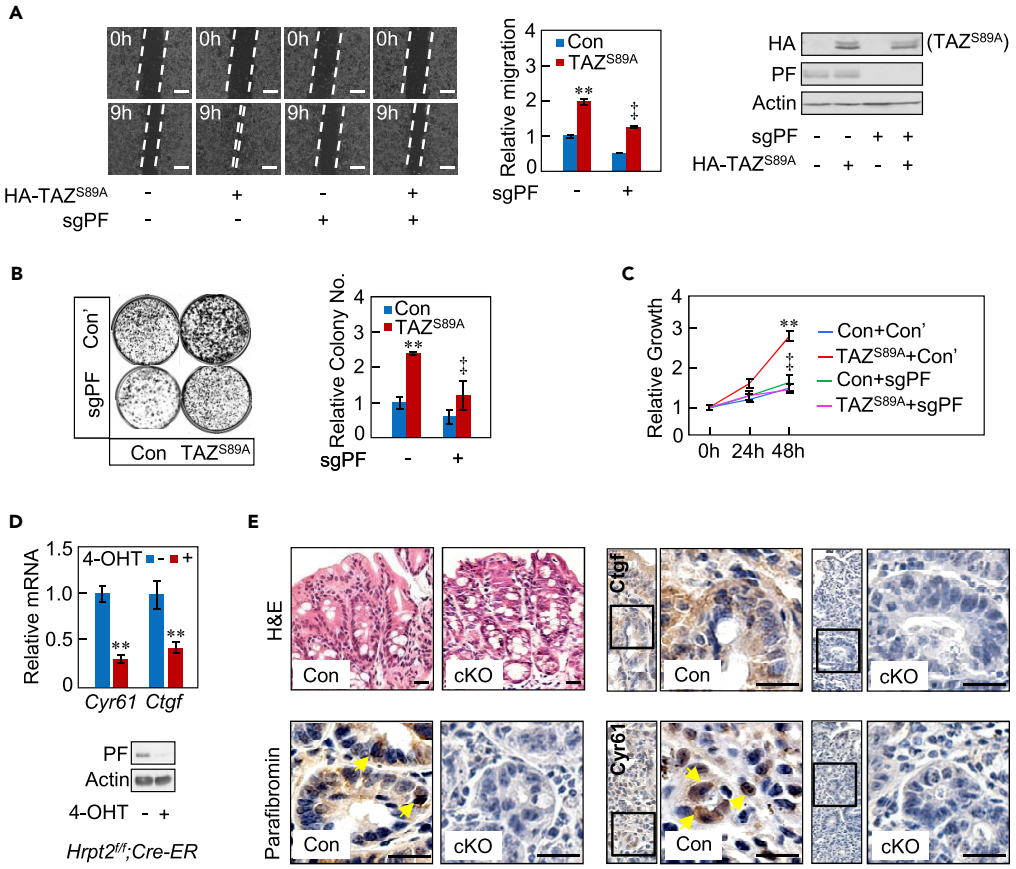

Figure 2. Enhancement of YAP/TAZ-Mediated Biological Actions by Parafibromin

(A) Wound healing assay was performed using AGS cells transiently transfected with an HA-TAZ^{S89A} vector or a control vector in the presence or absence of sgPF vector (left). The magnitudes of gap closures were quantified (middle). The levels of HA-TAZ^{S89A} and endogenous Parafibromin were determined by immunoblotting (right). Scale bars represent 100 μm.

(B) Colony formation assay of NIH3T3 cells transfected with the indicated plasmids.

(C) HEK293T cells were transfected with the indicated plasmids, and the cell proliferation was examined using 3-(4,5-dimethylthiazol-2-yl)-5-(3-carboxymethoxyphenyl)-2-(4-sulfophenyl)-2H-tetrazolium (MTS) assay 24 or 48 hr after transfection.

(D) qRT-PCR analysis of *Cyr61* and *Ctgf* mRNA expression in *Hrpt2*$^{flox/flox}$*;CAG-Cre-ER* MEFs with or without 4-hydroxytestosterone treatment. Parafibromin expression was also determined by immunoblotting.

(E) Immunohistochemistry of the colon from Parafibromin conditional knockout (cKO) mice (*Hrpt2*$^{flox/flox}$*;CAG-Cre-ER* mice) with or without tamoxifen treatment. Yellow arrows indicate positive staining (Parafibromin-expressing colon epithelial cells, left panel; Cyr61-expressingcolon epithelial cells, right panel). H&E staining (upper, left); Parafibromin staining (lower, left); Ctgf staining (upper, right); Cyr61 staining (lower, right). Scale bars represent 20 μm.

Error bars, mean ± SD; n = 3; **p < 0.01 versus control vector (A–C), or 4-OHT(−) (D); ‡p < 0.01 versus TAZ^{S89A} with control sgRNA (A–C). See also Figure S2.

(Zhang et al., 2009a, 2009b). Consistently, TAZ^{S89A} was found to stimulate the growth of NIH3T3 cells in a Parafibromin-dependent manner by colony formation assay (Figure 2B) or by examination of cell proliferation using the 3-(4,5-dimethylthiazol-2-yl)-5-(3-carboxymethoxyphenyl)-2-(4-sulfophenyl)-2H-tetrazolium (MTS) assay (Figure 2C). Acute deletion of the floxed *Parafibromin/Hrpt2* alleles in mouse embryonic fibroblasts (MEFs) also gave rise to a substantial reduction in the levels of TEAD-regulated *Cyr61* and *Ctgf* mRNAs (Figure 2D). Based on these results, we concluded that Parafibromin plays an important role in YAP/TAZ-mediated cell proliferation and cell motility.

To corroborate the functional interaction between Parafibromin and YAP/TAZ *in vivo*, we next investigated the expression of Parafibromin and YAP/TAZ-TEAD-regulated proteins in the mouse colon by immunohistochemistry after validation of the specificities of the anti-CTCF and anti-CYR61 antibodies by using specific siRNAs (Figure S2A). The YAP/TAZ targets Ctgf and Cyr61 were co-expressed with Parafibromin in

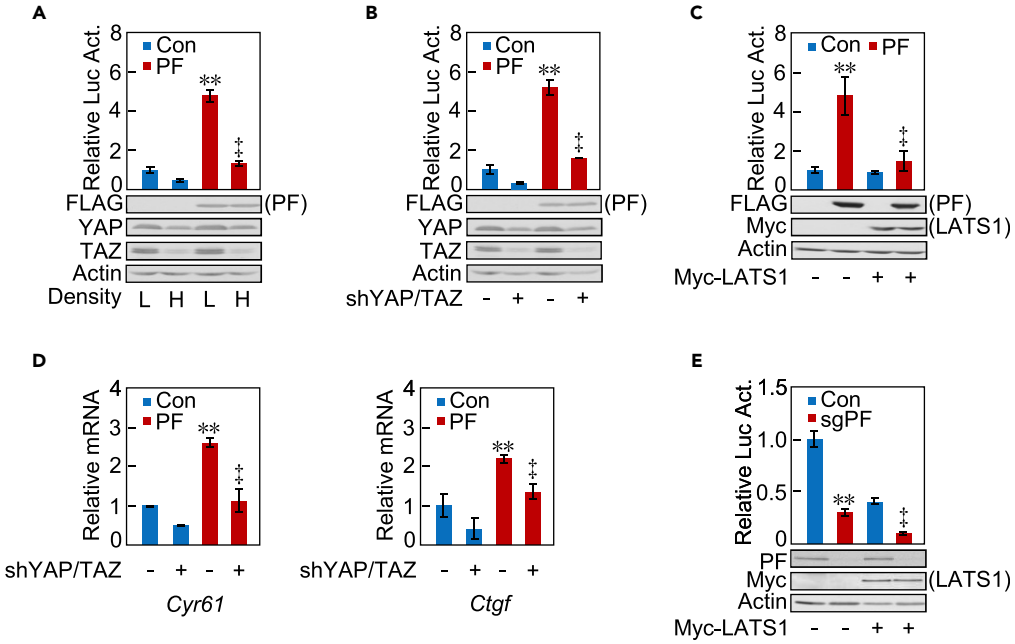

Figure 3. Effect of Hippo Signaling on Parafibromin-Mediated TEAD Activation

(A–C) HEK293T cells were transiently transfected with a TEAD luciferase reporter together with a Parafibromin (PF) or control empty vector (Con) at low (L) or high (H) cell density (A), in the presence or absence of a YAP/TAZ-specific shRNA vector (B), or in the presence or absence of Myc epitope-tagged LATS1 (Myc-LATS1) (C). Total cell lysates were subjected to luciferase assay or immunoblotting with indicated antibodies.

(D) qRT-PCR analysis of *Cyr61* and *Ctgf* mRNA expression in HEK293T cells transiently transfected with indicated plasmids.

(E) HEK293T cells were transiently transfected with a TEAD luciferase reporter together with indicated plasmids. Total cell lysates were subjected to luciferase assay or immunoblotting with indicated antibodies.

Error bars, mean ± SD; n = 3; **p < 0.01 versus control vector (A–E); ‡p < 0.01 versus PF with low cell density (A), PF with control vector (B and C), PF with control shRNA (D), or PF sgRNA with control vector (E).

See also Figure S3.

epithelial cells located in the bottom region of colonic crypts (Figure 2E). The expression of Ctgf and Cyr61 coincided with that of YAP/TAZ reported previously (Taniguchi et al., 2015). To further investigate *in vivo* roles of Parafibromin, we used Parafibromin conditional knockout mice (*Hrpt2*$^{flox/flox}$*;CAG-CreER mice*). The colonic mucosa had not undergone severe structural disintegration at 5 days after the onset of *Parafibromin/Hrpt2* deletion by tamoxifen treatment (Figure 2E). The Parafibromin-deleted colonic epithelium exhibited a marked reduction in the expression of Ctgf and Cyr61 (Figure 2E), indicating expression of YAP/TAZ targets is dependent on Parafibromin *in vivo*.

Effect of Hippo Signaling on Parafibromin-Mediated TEAD Activation

We next investigated the functional interplay between Parafibromin and the Hippo signaling pathway, which negatively regulates nuclear YAP/TAZ activities. To this end, we cultured HEK293T cells at a low cell density, which inactivates Hippo signaling, and at a high cell density, which activates Hippo signaling (Hergovich and Hemmings, 2009). As reported previously, the protein levels of YAP and TAZ were decreased at a high cell density, where activation of the TEAD reporter by Parafibromin was also diminished (Figure 3A). We then knocked down endogenous YAP and TAZ by specific shRNAs or overexpressed LATS1 or LATS2, which promotes degradation of YAP and TAZ by phosphorylating Ser127 and Ser89, respectively. Expectedly, YAP/TAZ knockdown or overexpression of LATS1/LATS2 attenuated Parafibromin-mediated TEAD reporter activation (Figures 3B, 3C, and S3A), which was concomitantly associated with reduced levels of *Cyr61* and *Ctgf* mRNAs (Figure 3D). Parafibromin knockout in conjunction with LATS1/LATS2 overexpression further diminished TEAD reporter activation compared with the effect of LATS1/2 overexpression alone (Figures 3E and S3B). Thus, Parafibromin-mediated potentiation of YAP/TAZ-TEAD activity was dampened by Hippo signal activation. This observation was consistent with the

notion that Hippo signal-mediated inhibition of nuclear YAP/TAZ translocalization impairs co-activator functions of YAP/TAZ, although the possibility that Parafibromin acts in parallel with the Hippo signal in TEAD regulation remains.

Physical Interaction of Parafibromin with YAP/TAZ

To gain insights into the mechanism underlying Parafibromin-mediated YAP/TAZ activation, we hypothesized that Parafibromin forms a physical complex with YAP or TAZ as is the case for other co-activators (Takahashi et al., 2011; Kikuchi et al., 2016). To test this idea, FLAG-tagged Parafibromin was transiently co-expressed with HA-tagged YAP1δ, YAP2δ, or TAZ in HEK293T cells and the cell lysates were subjected to immunoprecipitation with an anti-FLAG antibody. The results of the experiment revealed that the YAP isoforms and TAZ all bound to Parafibromin (Figure 4A). The complex formation was reproduced in HEK293A cells and AGS cells ectopically co-expressing Parafibromin and YAP or TAZ (Figures S4A and S4B). Furthermore, the co-immunoprecipitation experiment both ways with either an anti-Parafibromin antibody or anti-YAP/TAZ antibody detected the endogenous Parafibromin-YAP complex in HEK293T cells (Figure 4B). In this regard, we could not specify interaction of endogenous TAZ with endogenous Parafibromin because the molecular weight of TAZ is exactly the same as that of IgG heavy chain. Interestingly, YAP2δ, which possesses two WW domains, exhibited greater binding with Parafibromin than did YAP1δ and TAZ, which possess a single WW domain (Figure 4A). To test if the WW domain was essential for the interaction, we constructed YAP1δ$^{\Delta ww}$, which lacks the WW domain, and TAZ$^{ww\text{-}mut}$, which possesses a non-functional WW domain by double point mutations W152A/P155A (Diepenbruck et al., 2014). The WW domain mutations did not alter the subcellular localization of YAP/TAZ (data not shown). The results of a co-immunoprecipitation experiment revealed that neither YAP1δ$^{\Delta ww}$ nor TAZ$^{ww\text{-}mut}$ bound to Parafibromin (Figures 4C and 4D). Furthermore, both YAP1δ$^{\Delta ww}$ and TAZ$^{ww\text{-}mut}$ failed to stimulate TEAD reporter (Figures 4E and 4F) and YAP1δ$^{\Delta ww}$ did not induce endogenous YAP targets, *Cyr61* and *Ctgf* (Figure S4C). To test the involvement of the two WW domains, WW1 and WW2, in binding of YAP2 with Parafibromin, we disrupted WW1, WW2, or both by introducing point mutations in YAP2δ and conducted a co-immunoprecipitation experiment. As a result, WW1 was required for YAP2δ binding with Parafibromin, whereas WW2 was not (Figure 4G). The results of a TEAD reporter assay also showed that WW1-disrupted YAP2δ lost the ability to stimulate Parafibromin-dependent TEAD activation, whereas the WW2 disruption did not result in loss of the ability (Figure 4H). Hence, the WW domain, WW1 in YAP2, is critically involved in the interaction of YAP/TAZ with Parafibromin and the co-activator function of YAP/TAZ is activated through the interaction. Notably, however, Parafibromin binding with YAP2δ was diminished by inactivating WW2 (Figure 4G), suggesting an auxiliary role of WW2 in the interaction of YAP2δ with Parafibromin.

Differential Regulation of TAZ and YAP by Parafibromin

We next investigated the region(s) of Parafibromin required for YAP/TAZ binding. Co-immunoprecipitation analysis showed that the N-terminal half (residues 1–357) of Parafibromin is indispensable for YAP/TAZ binding, whereas the CDC73 core region, which consists of the C-terminal half (residues 358–531), is dispensable (Figures 5A and S5A). We previously reported that dephosphorylation of a cluster of the three tyrosine residues, Tyr290, Tyr293, and Tyr315, allows Parafibromin to interact with β-catenin and Gli1 (Takahashi et al., 2011; Kikuchi et al., 2016). We thus investigated the influence of the tyrosine phosphorylation status of Parafibromin on the Parafibromin-TAZ/YAP interaction. The results of a co-immunoprecipitation experiment revealed that the phosphorylation-resistant (PR) Parafibromin mutant (Parafibromin-Y290/293/315F) bound to TAZ substantially more strongly than did wild-type Parafibromin (Figure 5B). We next co-expressed Parafibromin, either wild type or PR, and TAZ in HEK293T cells and examined TEAD reporter activation. As a result, PR-Parafibromin markedly potentiated TAZ-mediated TEAD-reporter activation when compared with wild-type Parafibromin (Figure 5C). To determine the biological relevance of Parafibromin dephosphorylation in TAZ activity, we next performed a wound healing assay. The results showed that PR-Parafibromin stimulated TAZ^{S89A}-mediated gap closure more strongly than did wild-type Parafibromin (Figure 5D). In striking contrast to TAZ, interaction of Parafibromin with YAP1δ or YAP2δ was independent of the tyrosine phosphorylation status of Parafibromin (Figure 5E). Furthermore, wild-type Parafibromin enhanced YAP-dependent TEAD activation, whereas PR-Parafibromin failed to do so (Figure 5F).

We previously reported that protein tyrosine kinase 6 (PTK6, also known as BRK) and SHP2 are a kinase and a phosphatase that mediate tyrosine phosphorylation and dephosphorylation of Parafibromin, respectively

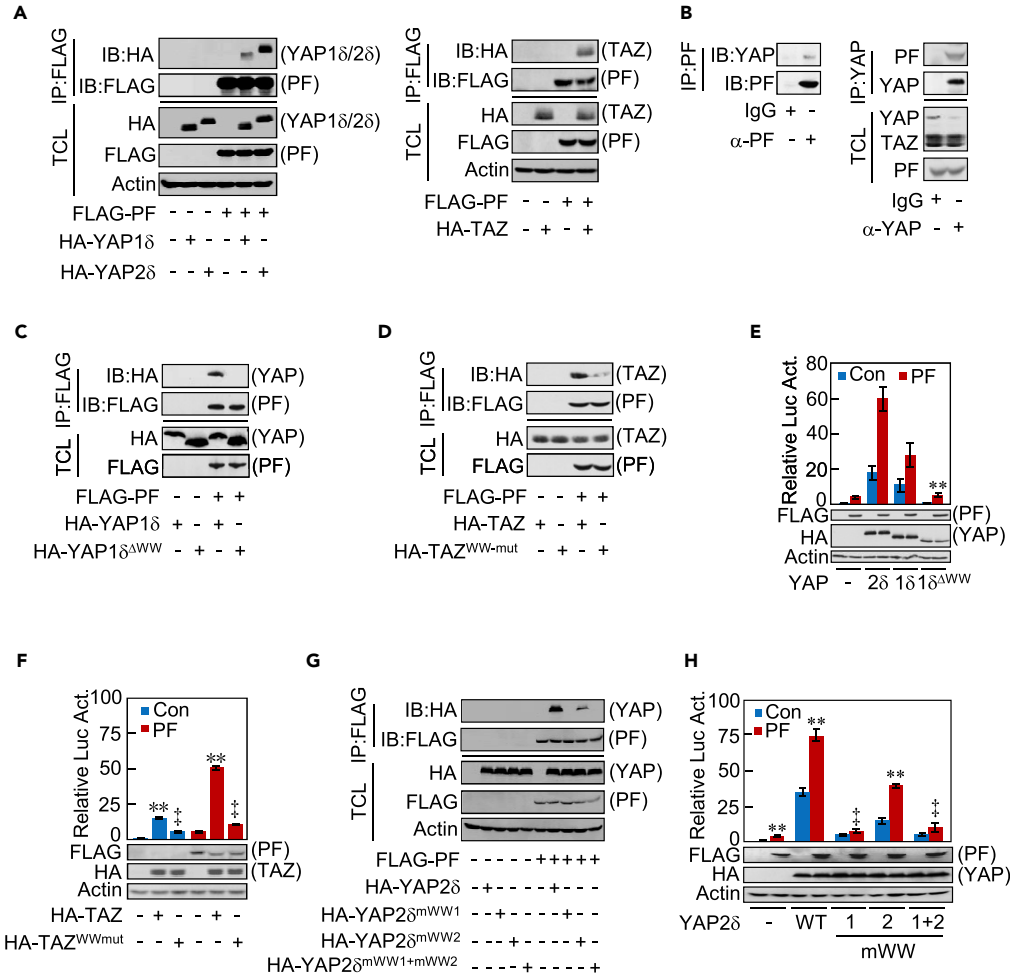

Figure 4. Physical Interaction between Parafibromin and YAP/TAZ

(A) HEK293T cells were transfected with indicated plasmids. Total cell lysates (TCLs) and anti-FLAG immunoprecipitates (IPs) from TCLs were analyzed by immunoblotting with anti-FLAG and anti-HA antibodies.

(B) An anti-PF (left) or anti-YAP/TAZ (right) immunoprecipitate from HEK293T cell lysates was analyzed by immunoblotting with anti-PF and anti-YAP/TAZ antibodies. Rabbit IgG was used for a negative control antibody of immunoprecipitation.

(C and D) HEK293T cells were transiently transfected with indicated plasmids. TCLs and anti-FLAG IPs from TCLs were analyzed by immunoblotting with anti-FLAG and anti-HA antibodies.

(E and F) HEK293T cells were transiently transfected with a TEAD luciferase reporter together with indicated plasmids. TCLs were subjected to luciferase assay and immunoblotting with the indicated antibodies.

(G) HEK293T cells were transiently transfected with indicated plasmids. TCLs and anti-FLAG IPs from TCLs were analyzed by immunoblotting with anti-FLAG and anti-HA antibodies.

(H) HEK293T cells were transiently transfected with a TEAD luciferase reporter together with indicated plasmids. TCLs were subjected to luciferase assay and immunoblotting with the indicated antibodies.

Error bars, mean ± SD; n = 3; **$p < 0.01$ versus YAP2δ with PF (E), control vector (F and H), PF with control vector (F), YAP2δ with control vector (H), or YAP2δ^{mWW2} with control vector (H); ‡$p < 0.01$ versus TAZ with control vector (F), TAZ with PF (F), or PF with YAP2δ (H).

See also Figure S4.

(Takahashi et al., 2011; Kikuchi et al., 2016), although the possibility exists that there are additional kinases/phosphatases involved in this process. To consolidate the importance of the tyrosine phosphorylation status of Parafibromin in TAZ binding, we transiently co-expressed Parafibromin and PTK6 in HEK293T cells and found that PTK6 markedly diminished Parafibromin-TAZ complex formation, which was concomitantly associated with reduced activation of the TEAD reporter (Figure 6A), whereas elevated PTK6 potentiated YAP-mediated TEAD activation (Figure 6B). Conversely, ectopic co-expression of SHP2 increased the amount of the Parafibromin-TAZ complex, which was associated with enhanced TEAD reporter activation

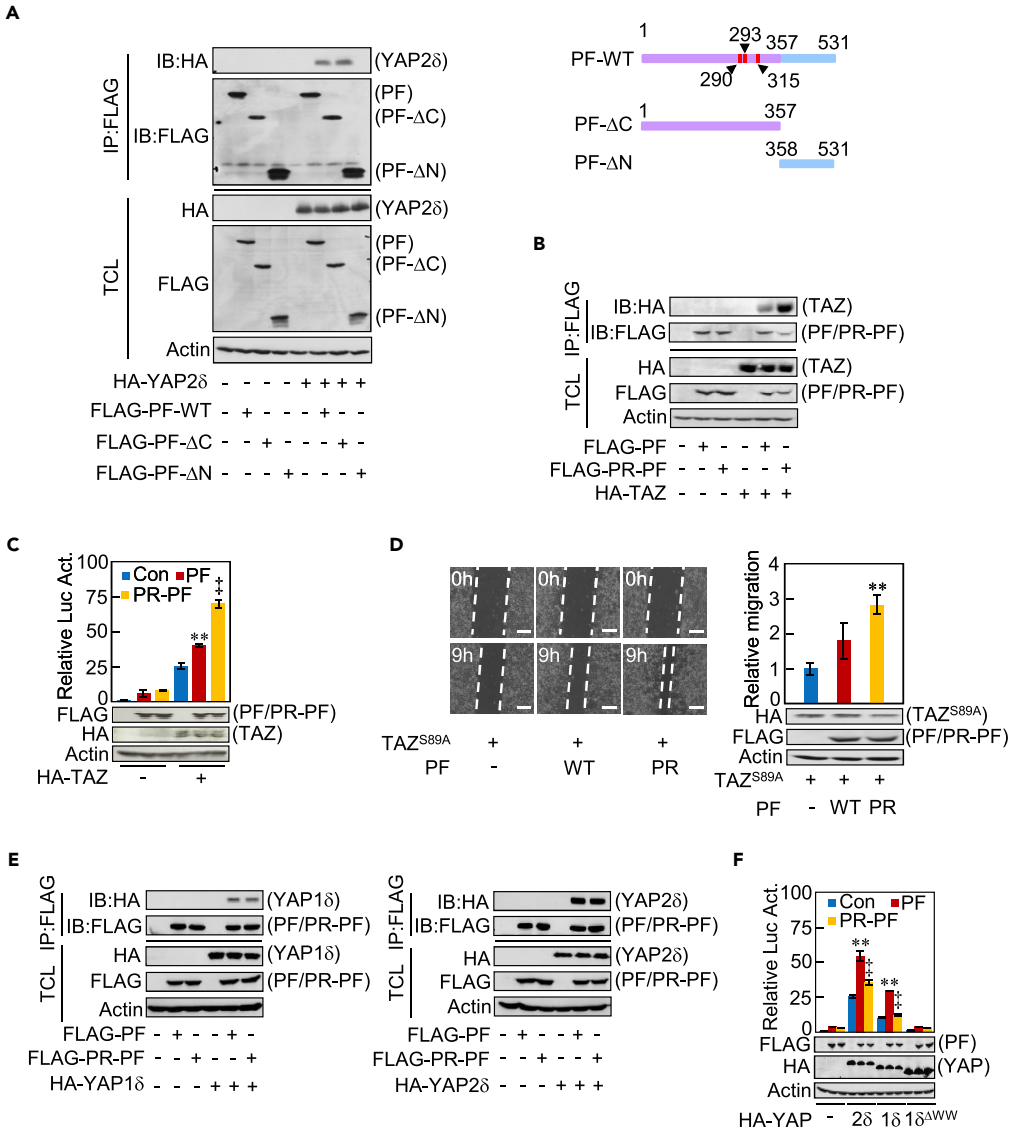

Figure 5. Differential Modes of Parafibromin Binding between YAP and TAZ

(A) HEK293T cells were co-transfected with indicated plasmids. Anti-FLAG IP from cell lysates and TCL were analyzed by immunoblotting with anti-FLAG and anti-HA antibodies (left). A schematic of Parafibromin and its deletion mutants (right). The three tyrosine dephosphorylation sites (Y290/293/315) are indicated.

(B) HEK293T cells were transfected with an FLAG-PF or FLAG-phosphoresistant (PR)-PF vector together an HA-TAZ vector. Anti-FLAG IP from cell lysates and TCL were subjected to immunoblotting with anti-FLAG and anti-HA antibodies.

(C) HEK293T cells were transfected with a TEAD luciferase reporter together with indicated plasmids. Total cell lysates were subjected to luciferase assay and immunoblotting analysis with indicated antibodies.

(D) Wound healing assay of AGS cells co-transfected with a TAZ^{S89A} vector and a PF or PR-PF vector. Scale bars represent 100 μm.

(E) HEK293T cells were transfected with indicated plasmids. TCLs and anti-FLAG immunoprecipitates from TCLs were subjected to immunoblotting with indicated antibodies.

(F) HEK293T cells were transfected with a TEAD luciferase reporter together with indicated plasmids. Total cell lysates were subjected to luciferase assay and immunoblotting with indicated antibodies.

Error bars, mean ± SD; n = 3; **p < 0.01 versus control vector with TAZ (C), PF with TAZ^{S89A} (D), control vector with YAP2δ (F), or control vector with YAP1δ (F); ‡p < 0.01 versus PF with TAZ (C), PF with YAP2δ (F), or PF with YAP1δ (F).

See also Figure S5.

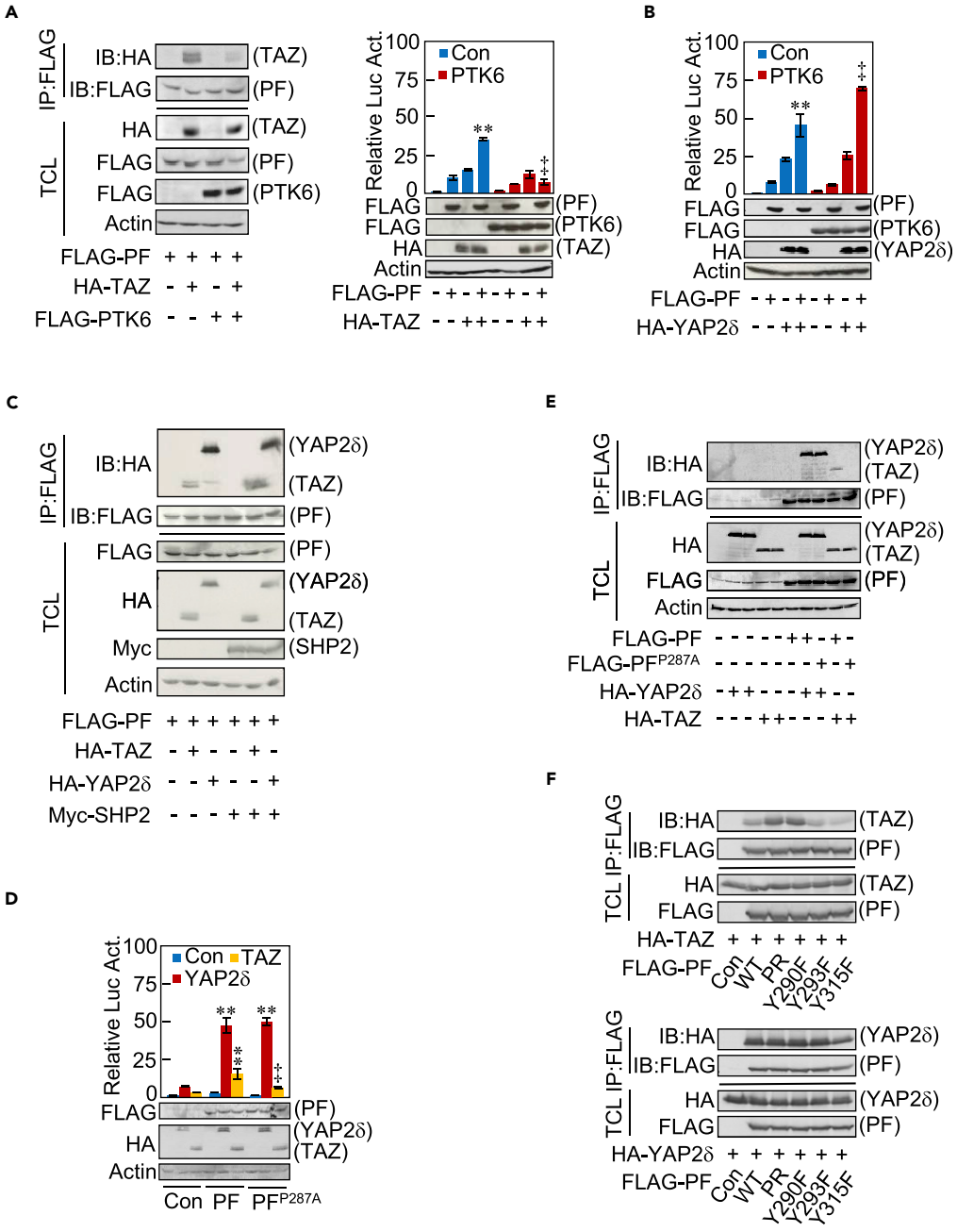

Figure 6. Inverse Regulation of YAP and TAZ Functions by Tyrosine Phosphorylation/Dephosphorylation of Parafibromin

(A) HEK293T cells were transfected with indicated plasmids. TCLs were subjected to a sequential immunoprecipitation-immunoblotting analysis with indicated antibodies (left) and luciferase assay (right).

(B) HEK293T cells were transiently transfected with a TEAD luciferase reporter together with indicated plasmids. The cell lysates were subjected to luciferase assay.

(C) HEK293T cells were transfected with indicated plasmids. Anti-FLAG IP from cell lysates and TCL were subjected to immunoblotting with indicated antibodies.

(D) HEK293T cells were transiently transfected with a TEAD luciferase reporter together with indicated plasmids. The cell lysates were subjected to luciferase assay.

(E and F) HEK293T cells were transfected with indicated plasmids. TCLs and anti-FLAG immunoprecipitates from TCLs were subjected to immunoblotting with indicated antibodies.

Error bars, mean ± SD; n = 3; **p < 0.01 versus control vector (A and B), control vector with YAP2δ (D), or control vector with TAZ (D); ‡p < 0.01 versus PF with TAZ (A and D), or PF with YAP2δ (B).

See also Figure S6.

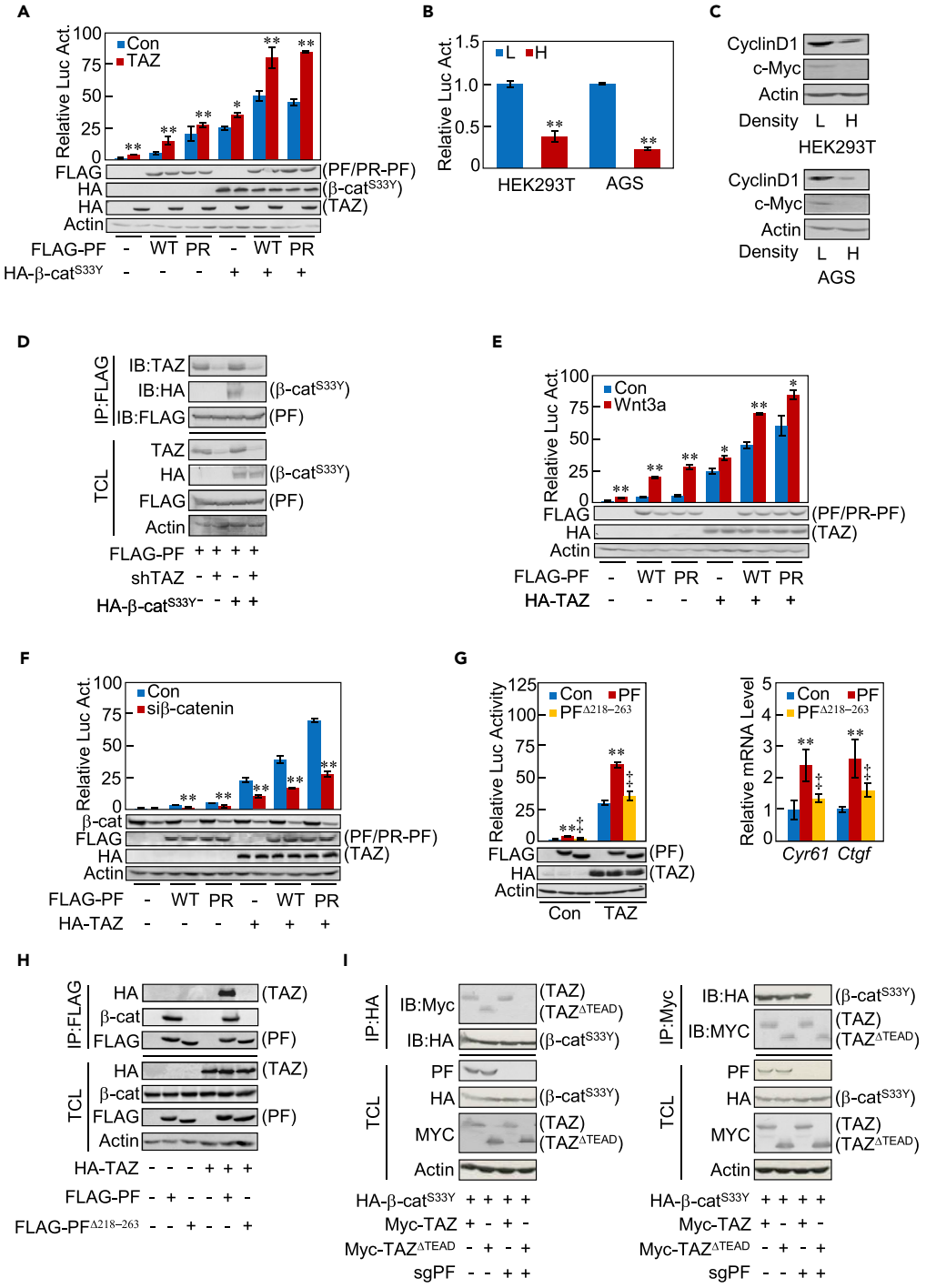

Figure 7. Synergism between Nuclear TAZ and the Wnt Signaling Pathway by Parafibromin

(A) HEK293T cells were transfected with a TOP-*tk* luciferase reporter together with indicated plasmids. TCLs were subjected to luciferase assay and immunoblotting analysis with indicated antibodies.

(B) HEK293T cells or AGS cells were cultured in a low-density (L) or a high-density (H) condition, and TOP-*tk* luciferase reporter activity was measured.

(C) Total cell lysates from (B) were subjected to immunoblotting.

(D) HEK293T cells were transfected with indicated plasmids. TCLs and the anti-FLAG immunoprecipitates were subjected to immunoblotting with the indicated antibodies.

Figure 7. *Continued*

(E) HEK293T cells were transfected with a TOP-*tk* luciferase reporter together with indicated plasmids. Cells were then treated with Wnt3a-conditioned medium or control medium. TCLs were subjected to luciferase assay and immunoblotting with the indicated antibodies.

(F) AGS cells were transfected with a TOP-*tk* luciferase reporter together with indicated plasmids. TCLs were subjected to luciferase assay and immunoblotting with the indicated antibodies.

(G) AGS cells were transfected with indicated vectors. Luciferase assay (left) and qRT-PCR (right) experiments were performed.

(H) AGS cells were transfected with indicated plasmids. Anti-FLAG immunoprecipitates from TCLs were subjected to immunoblotting with the indicated antibodies.

(I) An HA-β-catenin^{S33Y} vector was transfected together with a Myc-TAZ or Myc-TAZ$^{\Delta TEAD}$ vector into HEK293T cells, in which expression of endogenous Parafibromin was acutely inhibited by using CRISPR/CAS9-mediated gene knockout technique. Anti-HA (left) or anti-Myc (right) immunoprecipitates were prepared from TCLs and subjected to immunoblotting with the indicated antibodies. β-cat^{S33Y}; β-catenin^{S33Y}.

Error bars, mean ± SD; n = 3; *p < 0.05 versus control vector (A and E); **p < 0.01 versus control vector (A, E–G), low cell density (B), or control vector with TAZ (G); ‡p < 0.01 versus PF with control vector (G, left), PF (G, right), or PF with TAZ (G). See also Figure S7.

(Figures 6C and S6A). Although Parafibromin does not contain the PPxY sequence (where x is any amino acid), a canonical WW-binding sequence motif, it possesses a PPxY-related PxxY sequence at residues 287–290 (PAAY). Since Tyr290 is a major site of Parafibromin tyrosine phosphorylation (Takahashi et al., 2011), we mutated the PAAY sequence to AAAY (P287A) and performed a co-immunoprecipitation experiment and TEAD-luciferase assay using the Parafibromin mutant. Results of the experiment revealed that the PAAY sequence is crucial for Parafibromin-TAZ interaction and Parafibromin-mediated TEAD reporter activation, although the sequence was dispensable for the interaction of Parafibromin with YAP (Figures 6D and 6E). Since phosphorylation of Parafibromin on Tyr290 appeared to disable binding with the WW domain of TAZ, we also performed a co-immunoprecipitation experiment using AGS cells transiently co-transfected with a vector for wild-type, PR, Y290F, Y293F, or Y315F Parafibromin mutant and a YAP or TAZ vector. The results of the experiment revealed that, like PR-Parafibromin, Y290F but not Y293F or Y315F Parafibromin exhibited elevated TAZ binding, whereas these mutations did not influence the Parafibromin-YAP interaction. These results further support an important role of Tyr290 dephosphorylation in the interaction of Parafibromin with TAZ (Figure 6F).

TAZ Potentiates Nuclear Wnt Activation by Parafibromin

We next investigated whether Parafibromin coordinates YAP/TAZ with the morphogen signal. We conducted a Wnt reporter assay and found that TAZ strengthens Parafibromin-dependent Wnt activation (Figure 7A, compare lanes 7, 8, 10, and 12). On the other hand, YAP (YAP2δ) had little effect on Wnt activation by Parafibromin (Figure S7A, compare lanes 6, 8, 10, and 12). This was most probably because YAP fails to interact with the dephosphorylated Parafibromin/β-catenin complex, which directs Wnt activation. This idea was supported by the results of an experiment showing that ectopic SHP2, which tyrosine-dephosphorylates Parafibromin, dramatically elevated TAZ-dependent Wnt reporter activation but had little effect on YAP2δ-dependent Wnt reporter activation (Figure S7B). Conversely, elevated PTK6, which tyrosine-phosphorylates Parafibromin (Kikuchi et al., 2016), significantly promoted YAP2δ-induced Wnt reporter activation but had little effect on TAZ-induced Wnt reporter activation (Figure S7B). High-cell-density culture, which prevents nuclear accumulation of TAZ (Figure S7C) by stimulating the Hippo signal, gave rise to reduced Wnt reporter activity and decreased expression of Wnt targets such as Cyclin D1 and c-Myc (Figures 7B and 7C). β-Catenin has been shown to bind to the residues 218–263 of Parafibromin (Mosimann et al., 2006). Since YAP and TAZ also bind to the N-terminal region of Parafibromin, this led us to hypothesize that TAZ and β-catenin cooperatively interact with dephosphorylated Parafibromin. To test this idea, we performed a co-precipitation experiment using HEK293T cells treated with shTAZ in the presence or absence of stable β-catenin (the β-catenin^{S33Y} mutant) and found that knockdown of TAZ expression substantially reduced the amount of the Parafibromin/β-catenin complex (Figure 7D). In addition, treatment of HEK293T cells with a Wnt3a-conditioned medium potentiated TEAD reporter activity when compared with control medium treatment (Figures 7E and S7D). Also, treatment of cells with LiCl, which inhibits GSK-3β and thus activates Wnt signaling, enhanced TEAD reporter activation (Figures S7E and S7F). Since it has been reported that GSK3β destabilizes TAZ (Basu et al., 2013), LiCl might increase the level of TAZ and thereby potentiate the TEAD reporter. However, LiCl-treated cells did not show any substantial alterations in the levels of ectopically expressed TAZ protein. Since both endogenous and exogenous proteins should

undergo identical post-translational modifications in the cells, stimulation of the TEAD reporter by LiCl was unlikely to be due to the stabilization of TAZ. Conversely, knockdown of β-catenin in AGS cells diminished TEAD reporter activation (Figure 7F). Parafibromin$^{\Delta 218-263}$, a Parafibromin mutant lacking the β-catenin-binding region (residues 218–263), neither potentiated TEAD reporter activation nor induced *Ctgf* and *Cyr61* mRNAs (Figure 7G). These observations collectively support the idea that the Parafibromin-β-catenin interaction promotes Parafibromin-TAZ complex formation, which in turn strengthens TAZ-mediated TEAD activation. Notably, Parafibromin$^{\Delta 218-263}$ did not interact with TAZ. The result indicated that, in addition to the tyrosine-dephosphorylated PAAY sequence, the β-catenin-binding region (residues 218–263) is also required for the binding of Parafibromin with TAZ (Figure 7H). Since TAZ has been reported to directly bind to β-catenin via its TEAD-binding region (Imajo et al., 2012), we also wished to know whether TAZ and β-catenin directly interact with Parafibromin or whether the TAZ/β-catenin complex binds to Parafibromin via β-catenin as a bridging molecule. To this end, we constructed a TAZ mutant lacking the TEAD-binding region and performed a co-immunoprecipitation experiment in HEK293T cells in which *Parafibromin/Hrpt2* alleles had been acutely knocked out by the CRISPR/Cas9 system. As a result, β-catenin was co-precipitated with the mutant TAZ that cannot directly bind to β-catenin only when Parafibromin expression was rescued by cDNA expression (Figure 7I, left). Reciprocally, the mutant TAZ was co-precipitated with β-catenin only when Parafibromin expression was rescued (Figure 7I, right). Thus, TAZ and β-catenin bind to Parafibromin contiguously and cooperatively to form a stable heterotrimeric complex that mediates synergistic activation of Wnt- and TAZ-dependent genes.

DISCUSSION

We show in this work that the nuclear scaffold protein Parafibromin potentiates the co-activator functions of YAP and TAZ toward the TEAD transcription factors by forming a physical complex with YAP/TAZ via the WW domain. Previous studies have shown that the WW domain and the TEAD-binding domains are both required for growth stimulation and oncogenic transformation activities of YAP/TAZ (Zhao et al., 2009; Zhang et al., 2009a, 2009b), suggesting the presence of a WW-domain-binding protein that functionally collaborates with the YAP/TAZ-TEAD complex. Parafibromin fits nicely to the molecule assumed in these studies.

YAP and TAZ both possess the WW domain, a structural module involved in protein-protein interaction (Sudol, 1996; Reuven et al., 2015). YAP comprises two major isoforms, YAP1 and YAP2, differing in the number of WW domains owing to differential splicing. YAP1 possesses a single WW domain, WW1, which is highly homologous to the TAZ WW domain (~80% identity). YAP2 contains a second WW domain, WW2, in addition to WW1. WW2 shares only ~40% sequence identity with WW1. We found here that both YAP and TAZ bind to Parafibromin via the WW domain. As for YAP2, WW1 is necessary and sufficient for Parafibromin binding, although the presence of WW2 strengthens the interaction. Possibly, WW2 weakly interacts with Parafibromin via a region distinct from that recognized by WW1 and thereby reinforces the Parafibomin-WW1 interaction through avidity effects. The present study also revealed that the modes of Parafibromin binding are substantially different between TAZ and YAP. Parafibromin undergoes phosphorylation and dephosphorylation on Tyr290, Tyr293, and Tyr315 by kinases such as PTK6 and phosphatases such as SHP2, respectively (Kikuchi et al., 2016). YAP binds to both tyrosine-phosphorylated and tyrosine-dephosphorylated forms of Parafibromin, whereas TAZ specifically binds to dephosphorylated Parafibromin. Since the β-catenin-binding region of Parafibromin (residues 218–263) is commonly utilized for the interaction of Parafibromin with YAP and TAZ, there appears to be an additional site in Parafibromin that confers tyrosine-dephosphorylation-dependent binding to the WW domain of TAZ. Typically, the WW domain recognizes the non-phosphorylated PPxY motif and tyrosine phosphorylation in the PPxY motif often abolishes the WW domain binding. Although Parafibromin lacks the canonical PPxY motif, it possesses a PPxY-related PxxY (PAAY) sequence that contains Tyr290, one of three tyrosine phosphorylation sites, which plays the most important role in the Parafibromin/β-catenin interaction (Takahashi et al., 2011). It has been reported that the PxxY sequence can also interact with the WW domain (Lv et al., 2014), and indeed we found that stable binding with TAZ requires dephosphorylated PAAY in addition to the β-catenin-binding region of Parafibromin. Through the interaction, dephosphorylated Parafibromin stimulates the co-activator function of TAZ. On the other hand, Parafibromin interacts with YAP independently of tyrosine phosphorylation and, to our surprise, it is the tyrosine-phosphorylated form, but not the dephosphorylated form, of Parafibromin that stimulates the co-activator function of YAP upon binding. Accordingly, TAZ and YAP reciprocally activate TEAD-regulated genes depending on the tyrosine phosphorylation status of Parafibromin.

The present study adds YAP and TAZ to the list of transcriptional co-activators that are regulated by Parafibromin. We previously showed that tyrosine-dephosphorylated Parafibromin stimulates the Wnt effector/co-activator β-catenin and the Hedgehog effector/co-activator Gli1 in a mutually exclusive manner, whereas it synergistically stimulates β-catenin and the Notch effector NICD (Kikuchi et al., 2016). The present study extends the function of Parafibromin as a signal integrator and modulator by demonstrating that Parafibromin synergistically stimulates the co-activator functions of β-catenin and TAZ. The structural basis underpinning this functional cooperation is the formation of a heterotrimeric complex of β-catenin, TAZ, and tyrosine-dephosphorylated Parafibromin. Functional cross talk between YAP/TAZ and Wnt signaling has been described at multiple distinct levels (Varelas et al., 2010; Imajo et al., 2012). Although those studies indicate an inhibitory role of Wnt signaling on YAP/TAZ in the cytoplasm, the conclusion is not inconsistent with the results of our present work showing positive cooperativity between Wnt signaling and TAZ in the nucleus. Rather, these observations collectively raise the interesting possibility that Wnt antagonizes YAP/TAZ when the Hippo signal is on, whereas Wnt collaborates with TAZ when the Hippo signal is off. Such a mechanism should intensify the contrast with regard to the induction of Wnt- and TEAD-target genes upon on-off switching of the Hippo signal.

Although YAP and TAZ are not essential for homeostatic regulation of the intestinal epithelia (Hossain et al., 2007; Makita et al., 2008), elevated YAP provokes abnormal expansion of undifferentiated intestinal progenitor cells, indicating a growth promoting role of YAP (Camargo et al., 2007). Consistently, TAZ/YAP are critically involved in epithelial regeneration of damaged intestinal mucosa as well as deregulated proliferation of intestinal epithelial cells induced by *Apc* null mutation (Cai et al., 2010). Controversially, however, YAP can also inhibit intestinal regeneration following injury and counteracts Wnt-mediated intestinal hyperplasia (Barry et al., 2013). These observations suggest the presence of context-dependent regulation of YAP and/or TAZ activity that could even give rise to opposite biological outcomes. In this regard, the present study revealed that the co-activator functions of YAP and TAZ are inversely regulated by the tyrosine phosphorylation status of Parafibromin, which may differ among different cell types and also oscillate in response to altered extracellular environments such as cell density or the presence or absence of morphogens/mitogens/cytokines. It is therefore possible that intestinal mucosal damage induced by diverse stresses differentially activates kinases and phosphatases for Parafibromin, relative strengths of which determine the tyrosine phosphorylation status of Parafibromin. Prevalent accumulation of dephosphorylated Parafibromin may stimulate expansion of stem/progenitor cells and promote their subsequent differentiation through synergistic stimulation of TAZ and β-catenin by Parafibromin. On the other hand, predominance of tyrosine-phosphorylated Parafibromin may selectively stimulate YAP activity without co-stimulation of β-catenin, thereby impairing intestinal regeneration.

The present work uncovered that Parafibromin inversely stimulates the co-activator functions of YAP and TAZ depending on its tyrosine phosphorylation status, which is determined by the relative strength of Parafibromin kinase and phosphatase activities. Parafibromin also serves as a component of the PAF complex, which coordinates transcription with events downstream of RNA synthesis (Chaudhary et al., 2007). However, Parafibromin-mediated stimulation of the co-activator function of β-catenin does not require PAF complex formation (Takahashi et al., 2011). Also notably, the region of Parafibromin mediating interaction with β-catenin, Gli1, and YAP/TAZ is not conserved in Cdc73, the yeast ortholog of Parafibromin that comprises the PAF complex. It is therefore likely that functional interplay between Parafibromin and transcriptional co-activators is independent of PAF complex formation, although the conclusion requires further investigation.

METHODS

All methods can be found in the accompanying Transparent Methods supplemental file.

SUPPLEMENTAL INFORMATION

Supplemental Information includes Transparent Methods and seven figures and can be found with this article online at https://doi.org/10.1016/j.isci.2018.01.003.

ACKNOWLEDGMENTS

We thank Drs. Ryouhei Tsutsumi and Ximei Wu for help. This work was supported by Grant-in-Aids for Scientific Research on Innovative Area (16H06373; 16K15273) from the Ministry of Education, Culture, Sports,

Science, and Technology (MEXT), Japan (to M.H.); by Project for Cancer Research and Therapeutic Evolution (P-CREATE) (160200000291) from Japan Agency for Medical Research and Development (AMED), Japan (to M.H.); and by Grants-in-Aid of China Scholarship Council, China (to C.T., 201406320089).

AUTHOR CONTRIBUTIONS

C.T. performed all the experiments. A.T., I.K., and C.B. constructed plasmids. C.T. and M.H. analyzed the data. C.T. and M.H. designed the study and wrote the paper.

DECLARATION OF INTERESTS

The authors declare no competing interests.

Received: October 26, 2017
Revised: January 9, 2018
Accepted: January 23, 2018
Published: March 23, 2018; corrected online: April 4, 2018

REFERENCES

Barry, E.R., Morikawa, T., Butler, B.L., Shrestha, K., de la Rosa, R., Yan, K.S., Fuchs, C.S., Magness, S.T., Smits, R., Ogino, S., et al. (2013). Restriction of intestinal stem cell expansion and the regenerative response by YAP. Nature *493*, 106–110.

Basu, D., Reyes-Mugica, M., and Rebbaa, A. (2013). Histone acetylation-mediated regulation of the Hippo pathway. PLoS One *8*, e62478.

Cai, J., Zhang, N., Zheng, Y., de Wilde, R.F., Maitra, A., and Pan, D. (2010). The Hippo signaling pathway restricts the oncogenic potential of an intestinal regeneration program. Genes Dev. *24*, 2383–2388.

Camargo, F.D., Gokhale, S., Johnnidis, J.B., Fu, D., Bell, G.W., Jaenisch, R., and Brummelkamp, T.R. (2007). YAP1 increases organ size and expands undifferentiated progenitor cells. Curr. Biol. *17*, 2054–2060.

Carpten, J.D., Robbins, C.M., Villablanca, A., Forsberg, L., Presciuttini, S., Bailey-Wilson, J., Simonds, W.F., Gillanders, E.M., Kennedy, A.M., Chen, J.D., et al. (2002). *HRPT2*, encoding parafibromin, is mutated in hyperparathyroidism-jaw tumor syndrome. Nat. Genet. *32*, 676–680.

Chaudhary, K., Deb, S., Moniaux, N., Ponnusamy, M.P., and Batra, S.K. (2007). Human RNA polymerase II-associated factor complex: dysregulation in cancer. Oncogene *26*, 7499–7507.

Diepenbruck, M., Waldmeier, L., Ivanek, R., Berninger, P., Arnold, P., van Nimwegen, E., and Christofori, G. (2014). Tead2 expression levels control the subcellular distribution of Yap and Taz, zyxin expression and epithelial-mesenchymal transition. J. Cell Sci. *127*, 1523–1536.

Fan, R., Kim, N.G., and Gumbiner, B.M. (2013). Regulation of Hippo pathway by mitogenic growth factors via phosphoinositide 3-kinase and phosphoinositide-dependent kinase-1. Proc. Natl. Acad. Sci. USA *110*, 2569–2574.

Gumbiner, B.M., and Kim, N.G. (2014). The Hippo-YAP signaling pathway and contact inhibition of growth. J. Cell Sci. *127*, 709–717.

Guo, L., and Teng, L. (2015). YAP/TAZ for cancer therapy: opportunities and challenges (review). Int. J. Oncol. *46*, 1444–1452.

Hansen, C.G., Moroishi, T., and Guan, K.L. (2015). YAP and TAZ: a nexus for Hippo signaling and beyond. Trends Cell Biol. *25*, 499–513.

Hergovich, A., and Hemmings, B.A. (2009). Mammalian NDR/LATS protein kinases in hippo tumor suppressor signaling. Biofactors *35*, 338–345.

Hoshino, M., Qi, M.L., Yoshimura, N., Miyashita, T., Tagawa, K., Wada, Y., Enokido, Y., Marubuchi, S., Harjes, P., Arai, N., et al. (2006). Transcriptional repression induces a slowly progressive atypical neuronal death associated with changes of YAP isoforms and p73. J. Cell Biol. *172*, 589–604.

Hossain, Z., Ali, S.M., Ko, H.L., Xu, J., Ng, C.P., Guo, K., Qi, Z., Ponniah, S., Hong, W., and Hunziker, W. (2007). Glomerulocystic kidney disease in mice with a targeted inactivation of Wwtr1. Proc. Natl. Acad. Sci. USA *104*, 1631–1636.

Hsu, Y.L., Hung, J.Y., Chou, S.H., Huang, M.S., Tsai, M.J., Lin, Y.S., Chiang, S.Y., Ho, Y.W., Wu, C.Y., and Kuo, P.L. (2015). Angiomotin decreases lung cancer progression by sequestering oncogenic YAP/TAZ and decreasing Cyr61 expression. Oncogene *34*, 4056–4068.

Imajo, M., Miyatake, K., Iimura, A., Miyamoto, A., and Nishida, E. (2012). A molecular mechanism that links Hippo signalling to the inhibition of Wnt/β-catenin signalling. EMBO J. *31*, 1109–1122.

Kikuchi, I., Takahashi-Kanemitsu, A., Sakiyama, N., Tang, C., Tang, P.J., Noda, S., Nakao, K., Kassai, H., Sato, T., Aiba, A., et al. (2016). Dephosphorylated parafibromin is a transcriptional coactivator of the Wnt/Hedgehog/Notch pathways. Nat. Commun. *7*, 12887.

Lv, Y., Zhang, K., and Gao, H. (2014). Paip1, an effective stimulator of translation initiation, is targeted by WWP2 for ubiquitination and degradation. Mol. Cell. Biol. *34*, 4513–4522.

Makita, R., Uchijima, Y., Nishiyama, K., Amano, T., Chen, Q., Takeuchi, T., Mitani, A., Nagase, T., Yatomi, Y., Aburatani, H., et al. (2008). Multiple renal cysts, urinary concentration defects, and pulmonary emphysematous changes in mice lacking TAZ. Am. J. Physiol. Renal Physiol. *294*, F542–F553.

Morin-Kensicki, E.M., Boone, B.N., Howell, M., Stonebraker, J.R., Teed, J., Alb, J.G., Magnuson, T.R., O'Neal, W., and Milgram, S.L. (2006). Defects in yolk sac vasculogenesis, chorioallantoic fusion, and embryonic axis elongation in mice with targeted disruption of Yap65. Mol. Cell. Biol. *26*, 77–87.

Mosimann, C., Hausmann, G., and Basler, K. (2006). Parafibromin/Hyrax activates Wnt/Wg target gene transcription by direct association with β-catenin/Armadillo. Cell *125*, 327–341.

Mosimann, C., Hausmann, G., and Basler, K. (2009). The role of Parafibromin/Hyrax as a nuclear Gli/Ci-interacting protein in Hedgehog target gene control. Mech. Dev. *126*, 394–405.

Pan, D. (2010). The hippo signaling pathway in development and cancer. Dev. Cell *19*, 491–505.

Pfleger, C.M. (2017). The Hippo pathway: a master regulatory network important in development and dysregulated in disease. Curr. Top. Dev. Biol. *123*, 181–228.

Pobbati, A.V., and Hong, W. (2013). Emerging roles of TEAD transcription factors and its coactivators in cancers. Cancer Biol. Ther. *14*, 390–398.

Reuven, N., Shanzer, M., and Shaul, Y. (2015). Tyrosine phosphorylation of WW proteins. Exp. Biol. Med. *240*, 375–382.

Rozenblatt-Rosen, O., Hughes, C.M., Nannepaga, S.J., Shanmugam, K.S., Copeland, T.D., Guszczynski, T., Resau, J.H., and Meyerson, M. (2005). The parafibromin tumor suppressor protein is part of a human Paf1 complex. Mol. Cell. Biol. *25*, 612–620.

Shimomura, T., Miyamura, N., Hata, S., Miura, R., Hirayama, J., and Nishina, H. (2014). The PDZ-binding motif of Yes-associated protein is

required for its co-activation of TEAD-mediated *CTGF* transcription and oncogenic cell transforming activity. Biochem. Biophys. Res. Commun. *443*, 917–923.

Sudol, M. (1996). Structure and function of the WW domain. Prog. Biophys. Mol. Biol. *65*, 113–132.

Takahashi, A., Tsutsumi, R., Kikuchi, I., Obuse, C., Saito, Y., Seidi, A., Karisch, R., Fernandez, M., Cho, T., Ohnishi, N., et al. (2011). SHP2 tyrosine phosphatase converts parafibromin/Cdc73 from a tumor suppressor to an oncogenic driver. Mol. Cell *43*, 45–56.

Taniguchi, K., Wu, L.W., Grivennikov, S.I., de Jong, P.R., Lian, I., Yu, F.X., Wang, K., Ho, S.B., Boland, B.S., Chang, J.T., et al. (2015). A gp130-Src-YAP module links inflammation to epithelial regeneration. Nature *519*, 57–62.

Tsutsumi, R., Masoudi, M., Takahashi, A., Fujii, Y., Hayashi, T., Kikuchi, I., Satou, Y., Taira, M., and Hatakeyama, M. (2013). YAP and TAZ, Hippo signaling targets, act as a rheostat for nuclear SHP2 function. Dev. Cell *26*, 658–665.

Varelas, X., Miller, B.W., Sopko, R., Song, S., Gregorieff, A., Fellouse, F.A., Sakuma, R., Pawson, T., Hunziker, W., McNeill, H., et al. (2010). The Hippo pathway regulates Wnt/β-catenin signaling. Dev. Cell *18*, 579–591.

Wang, K., Degerny, C., Xu, M., and Yang, X.J. (2009). YAP, TAZ, and Yorkie: a conserved family of signal-responsive transcriptional coregulators in animal development and human disease. Biochem. Cell Biol. *87*, 77–91.

Wang, P.F., Tan, M.H., Zhang, C., Morreau, H., and Teh, B.T. (2005). HRPT2, a tumor suppressor gene for hyperparathyroidism-jaw tumor syndrome. Horm. Metab. Res. *37*, 380–383.

Webb, C., Upadhyay, A., Giuntini, F., Eggleston, I., Furutani-Seiki, M., Ishima, R., and Bagby, S. (2011). Structural features and ligand binding properties of tandem WW domains from YAP and TAZ, nuclear effectors of the Hippo pathway. Biochemistry *50*, 3300–3309.

Yart, A., Gstaiger, M., Wirbelauer, C., Pecnik, M., Anastasiou, D., Hess, D., and Krek, W. (2005). The *HRPT2* tumor suppressor gene product parafibromin associates with human PAF1 and RNA polymerase II. Mol. Cell. Biol. *25*, 5052–5060.

Yu, F.X., Zhao, B., and Guan, K.L. (2015). Hippo Pathway in organ size control, tissue homeostasis, and cancer. Cell *163*, 811–828.

Yu, F.X., Zhao, B., Panupinthu, N., Jewell, J.L., Lian, I., Wang, L.H., Zhao, J., Yuan, H., Tumaneng, K., Li, H., et al. (2012). Regulation of the Hippo-YAP pathway by G-protein-coupled receptor signaling. Cell *150*, 780–791.

Zhang, H., Liu, C.Y., Zha, Z.Y., Zhao, B., Yao, J., Zhao, S., Xiong, Y., Lei, Q.Y., and Guan, K.L. (2009a). TEAD transcription factors mediate the function of TAZ in cell growth and epithelial-mesenchymal transition. J. Biol. Chem. *284*, 13355–13362.

Zhang, X., Milton, C.C., Humbert, P.O., and Harvey, K.F. (2009b). Transcriptional output of the Salvador/warts/hippo pathway is controlled in distinct fashions in *Drosophila melanogaster* and mammalian cell lines. Cancer Res. *69*, 6033–6041.

Zhao, B., Wei, X., Li, W., Udan, R.S., Yang, Q., Kim, J., Xie, J., Ikenoue, T., Yu, J., Li, L., et al. (2007). Inactivation of YAP oncoprotein by the Hippo pathway is involved in cell contact inhibition and tissue growth control. Genes Dev. *21*, 2747–2761.

Zhao, B., Kim, J., Ye, X., Lai, Z.C., and Guan, K.L. (2009). Both TEAD-binding and WW domains are required for the growth stimulation and oncogenic transformation activity of yes-associated protein. Cancer Res. *69*, 1089–1098.

Zhao, B., Li, L., Tumaneng, K., Wang, C.Y., and Guan, K.L. (2010). A coordinated phosphorylation by Lats and CK1 regulates YAP stability through $SCF^{\beta\text{-}TRCP}$. Genes Dev. *24*, 72–85.

Zhou, Y., Huang, T., Cheng, A.S., Yu, J., Kang, W., and To, K.F. (2016). The TEAD family and its oncogenic role in promoting tumorigenesis. Int. J. Mol. Sci. *17*, E138.

ISCI, Volume *1*

Supplemental Information

Transcriptional Co-activator Functions of YAP and TAZ Are Inversely Regulated by Tyrosine Phosphorylation Status of Parafibromin

Chao Tang, Atsushi Takahashi-Kanemitsu, Ippei Kikuchi, Chi Ben, and Masanori Hatakeyama

Supplemental Information

Supplemental Figures

Figure S1

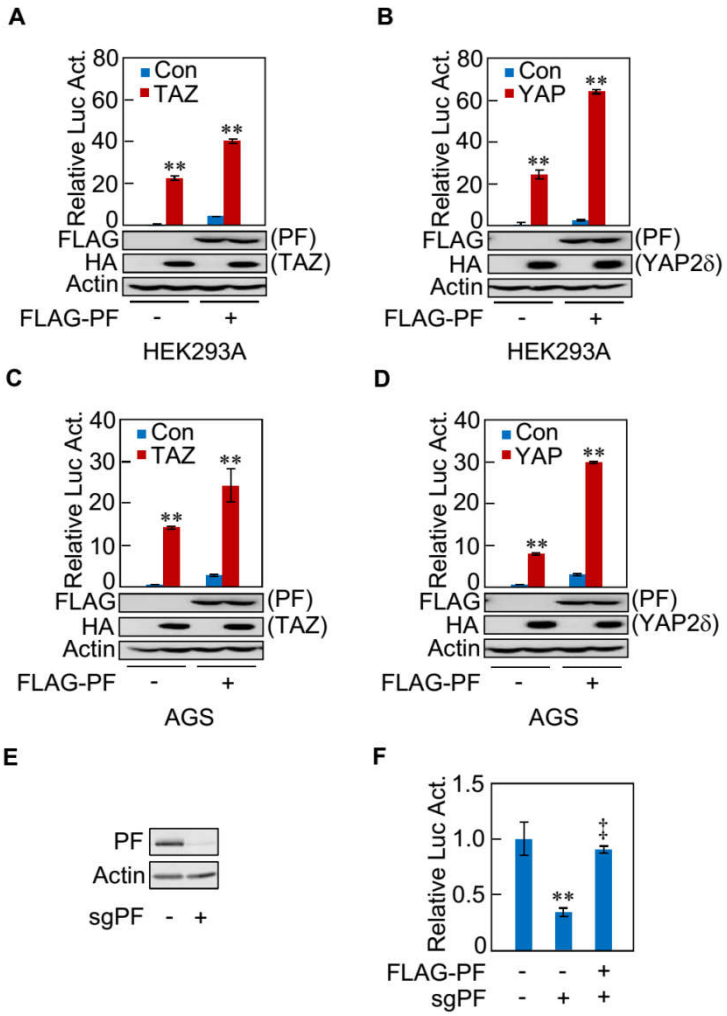

Figure S1. Related to Figure 1. Potentiation of the transcriptional co-activator activity of YAP and TAZ toward TEAD by Parafibromin

(A and B) HEK293A cells were transfected with indicated vectors together with reporter plasmids. Total cell lysates were subjected to immunoblotting with indicated antibodies.

(C and D) AGS cells were transfected with indicated vectors together with reporter plasmids. Total cell lysates were subjected to immunoblotting with indicated antibodies.

(E) HEK293T cells were transfected with indicated vectors. Total cell lysates were subjected to immunoblotting with indicated antibodies.

(F) HEK293T cells were transiently transfected with a TEAD luciferase reporter together with a sgPF vector together with or without PF vector.

Error bars, mean ± SD; n = 3; **p<0.01 versus control vector (A-D, F), or PF with control vector (A-D); ‡p<0.01 versus PF sgRNA with control vector (F).

Figure S2

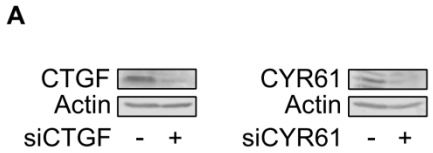

Figure S2. Related to Figure 2. Enhancement of YAP/TAZ-mediated biological actions by Parafibromin

(A) HEK293T cells were transiently transfected with *Ctgf*-specific siRNA, *Cyr61*-specific siRNA, or control siRNA. Total cell lysates were subjected to an immunoblotting with indicated antibodies.

Figure S3

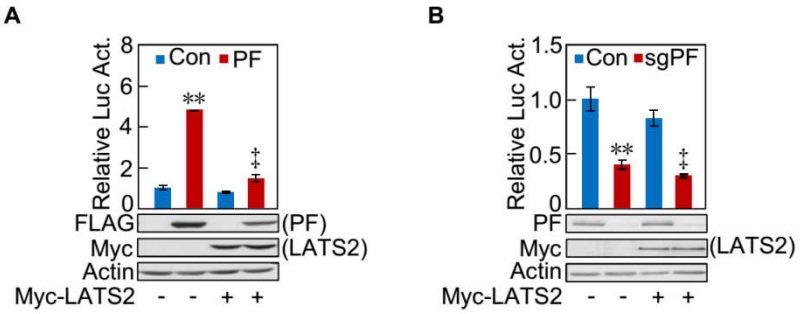

Figure S3. Related to Figure 3. Effect of Hippo signaling on Parafibromin-mediated TEAD activation

(A) HEK293T cells were transiently transfected with a TEAD luciferase reporter together with Parafibromin vector or a control empty vector in the presence or absence of a Myc-LATS2 vector. Total cell lysates were subjected to a luciferase assay or an immunoblotting with indicated antibodies.

(B) HEK293T cells were transiently transfected with a TEAD luciferase reporter together with Parafibromin-specific sgRNA vector or a control empty vector in the presence or absence of a Myc-LATS2 vector. Total cell lysates were subjected to a luciferase assay or an immunoblotting with indicated antibodies.

Error bars, mean ± SD; n = 3; **p<0.01 versus control vector (A and B); ‡p<0.01 versus PF with control vector (A), or PF sgRNA with control vector (B).

Figure S4

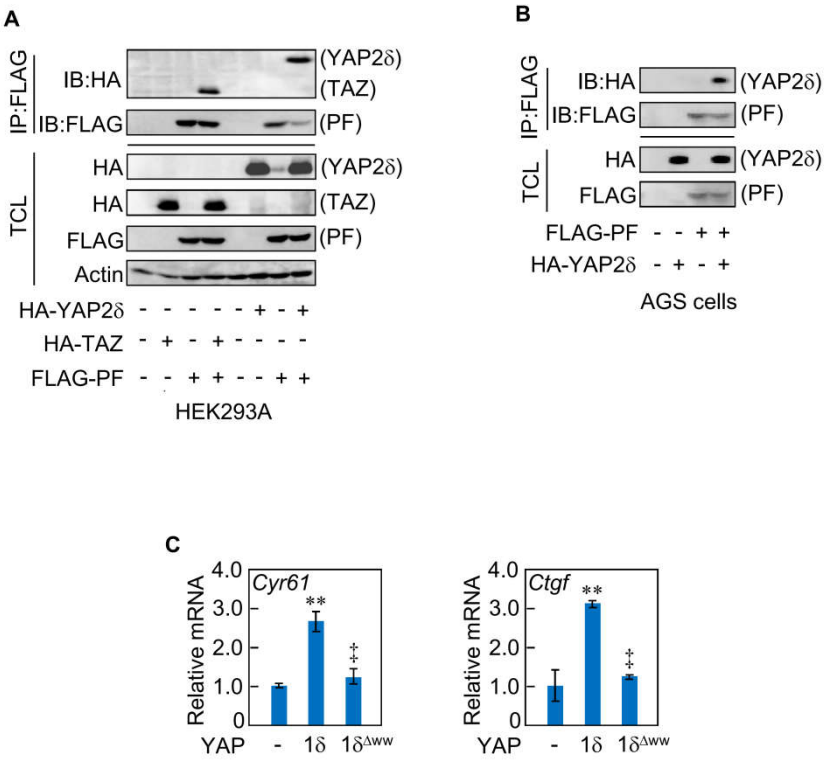

Figure S4. Related to Figure 4. Physical interaction between Parafibromin and YAP/TAZ

(A) HEK293A cells were transfected with expression vectors of either HA-YAP2δ or HA-TAZ, together with that of FLAG-Parafibromin. Anti-FLAG IP from cell lysates and TCL were analyzed by immunoblotting with anti-FLAG and anti-HA antibodies.

(B) AGS cells were transfected with expression vectors of HA-YAP2δ and FLAG-Parafibromin. Anti-Flag IP from cell lysates and TCL were analyzed by immunoblotting with anti-FLAG and anti-HA antibodies.

(C) qRT-PCR analysis of Cyr61 and Ctgf mRNA expression in HEK293T cells transiently transfected with a HA-YAP1δ, HA-YAP1$\delta^{\Delta ww}$ or control vector.

Error bars, mean ± SD; n = 3; **p<0.01 versus control vector; ‡p<0.01 versus YAP1δ.

Figure S5

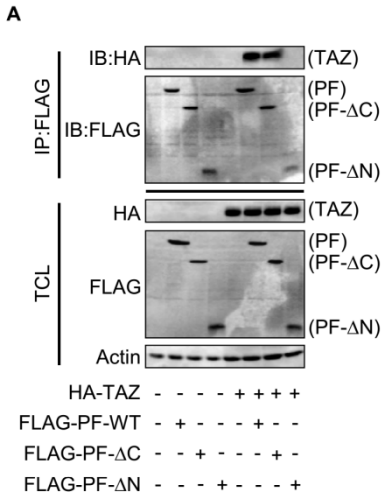

Figure S5. Related to Figure 5. Potentiation of transcriptional co-activator TAZ by tyrosine dephosphorylation of Parafibromin

(A) HEK293T cells were transfected with expression vectors of FLAG-Parafibromin, FLAG-Parafibromin-ΔC or FLAG-Parafibromin-ΔN, together with that of HA-TAZ. Anti-Flag IP from cell lysates and TCL were analyzed by immunoblotting with anti-FLAG and anti-HA antibodies.

Figure S6

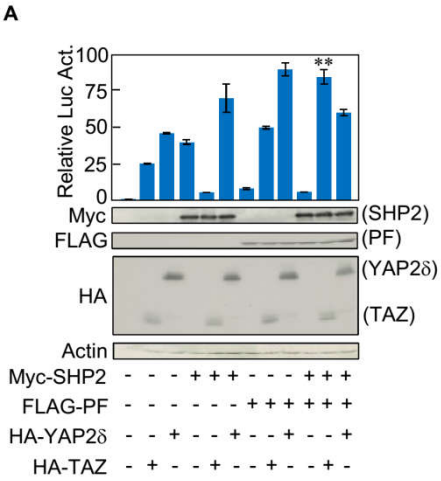

Figure S6. Related to Figure 6. Differential regulation of YAP by tyrosine dephosphorylation of Parafibromin

(A) HEK293T cells were transfected with indicated vectors together with a TEAD reporter plasmid. Total cell lysates were subjected to immunoblotting with indicated antibodies.

Error bars, mean ± SD; n = 3; **p<0.01 versus PF with TAZ.

Figure S7

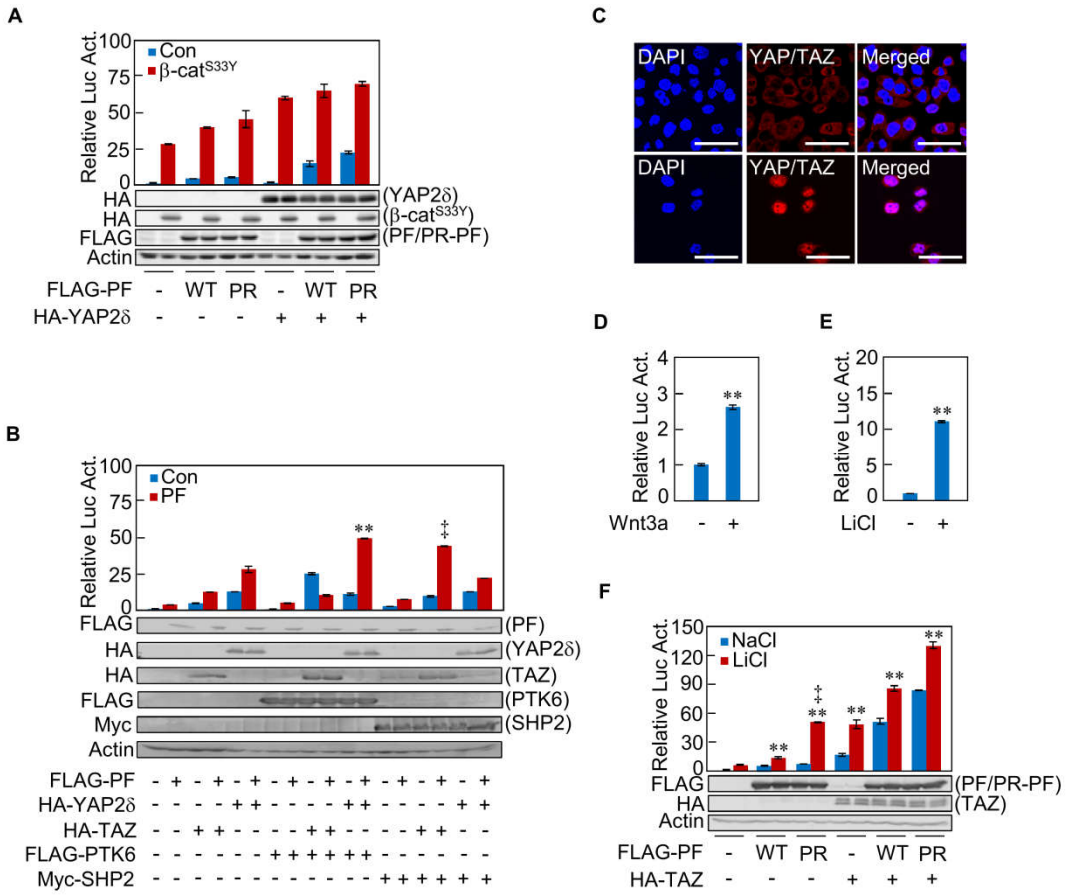

Figure S7. Related to Figure 7. Synergism between nuclear TAZ and Wnt signaling pathways by Parafibromin

(A) HEK293T cells were transfected with a TOP-*tk* luciferase reporter together with a FLAG-PF or FLAG-PR-PF vector with an HA-β-catenin^{S33Y} vector and/or an HA-YAP2δ vector. TCLs were subjected to luciferase assay and immunoblotting analysis with indicated antibodies.

(B) HEK293T cells were transfected with a FLAG-PF vector together with an HA-YAP2δ vector or an HA-TAZ vector with a FLAG-PTK6 vector or a Myc-SHP2 vector. TCLs were subjected to luciferase assay and immunoblotting analysis with indicated antibodies.

(C) AGS cells were seeded at high (upper) or low (lower) cell density, and cultured for 24 h. Immunnostaining was performed with indicated antibody and DAPI. Scale bars, 50 μm.

(D and E) HEK293T cells were transfected with a TOP-*tk* luciferase reporter. Cells were then treated with Wnt3a-conditioned medium or control medium(C), or treated with LiCl or NaCl (D).

(F) HEK293T cells were transfected with a TOP-*tk* luciferase reporter together with a FLAG-PF or FLAG-PR-PF and/or an HA-TAZ vector. Cells were then treated with LiCl or NaCl. TCLs were subjected to luciferase assay and immunoblotting with the indicated antibodies.

Error bars, mean ± SD; n = 3; **p <0.01 versus PF with YAP2δ (B), control medium (D), NaCl (E), PF (F), PR-PF (F), TAZ (F), TAZ with PF (F) or TAZ with PR-PF (F); ‡p <0.01 versus PF with TAZ (B) or PF with LiCl (F).

Transparent Methods

Cell culture and transfections

HEK293T, HEK293A, NIH3T3 and *Hrpt2*$^{flox/flox}$*;CAG-CreER* MEF cells were cultured in Dulbecco's modified Eagle's medium (DMEM) supplemented with 10% fetal bovine serum (FBS). AGS cells were cultured in RPMI 1640 medium with 10% FBS. To activate endogenous Wnt signaling, HEK293T cells were treated with 25 mM LiCl, which inhibits GSK-3β and prevents β-catenin degradation. Transient transfection was carried out by using Lipofectamine reagent (Invitrogen) with Plus reagent (Invitrogen) for HEK293T, HEK293A and NIH3T3 cells, and using Lipofectamine 2000 reagent (Invitrogen) for AGS cells. *Hrpt2*$^{flox/flox}$*;CAG-CreER* MEFs were treated with 500 nM 4-OHT (Sigma) for 72 h to conditionally delete *Hrpt2* alleles.

Plasmids

The expression vectors for N-terminally FLAG-tagged wild-type Parafibromin, phospho-resistant Y290/293/315F Parafibromin (PR-Parafibromin), Y290F Parafibromin, Y293F Parafibromin, Y315F Parafibromin and Myc-tagged human SHP2 were described previously (Takahashi et al., 2011). The expression vector of a PxxY motif deficient mutant of FLAG-tagged Parafibromin, FLAG-tagged Parafibromin (P287A), was generated from the FLAG-tagged wild-type Parafibromin expression vector by site-directed mutagenesis. The cDNA encoding human PTK6 was cloned into the pRc/CMV vector (Invitrogen). The cDNA encoding hemagglutinin (HA)-tagged human TAZ was amplified from AGS cells with an HA-tag sequence in 5' and cloned into the pcDNA3 vector as previously described (Tsutsumi et al., 2013). The cDNA encoding HA-tagged human YAP isoforms were amplified from AGS cells with an HA-tag sequence in 5' and cloned into the pSP65-SRα vector. The WW domain-deleted mutant was generated from the expression vector YAP1δ isoform. Expression vectors of a WW domain-deficient mutant of TAZ, HA-TAZ WW domain-mutant (W152A/P155A), and a phosphorylation-resistant mutant of TAZ (TAZ-S89A) were generated from the HA-TAZ expression vector by site-directed mutagenesis. Expression vectors of either WW domain-deficient mutant of YAP2δ, HA-YAP2δ WW1 domain-mutant (W199A/P202A) and WW2 domain-mutant (W258A/P261A), and a double WW domains-deficient mutant of YAP2δ, HA-YAP2δ (W199A/P202A, W258A/P261A) were generated from the HA-YAP2δ expression vector by site-directed mutagenesis. The expression vector for HA-tagged β-catenin (S33Y) was generated from the expression vector for HA-β-catenin by introducing a point mutation (S33Y) by site-directed mutagenesis according to the method described previously (Takahashi et al., 2011). Wnt-responsive Top-*tk* and YAP/TAZ-responsive 8×GT TEAD-luciferase reporter plasmids have been described previously (Tsutsumi et al., 2013). Expression vectors of shRNA for human TAZ and human YAP were designed as pSUPER-based plasmids that target sequences of 5'-ACGTTGACTTAGGAACTTT-3', and 5'-GACATCTTCTGGTCAGAGA-3', respectively, as described previously (Tsutsumi et al., 2013).

CRISPR/Cas9 to Parafibromin/CDC73 construction and transfection

Expression vectors of sgRNA for human Parafibromin/CDC73 was designed as pX330-based plasmids that target sequences of 5'-CACCGAAGAAGGAGATTGTGGTGA-3'(#1), 5'-CACCGGGAGACGAAGTGATCTTCG-3'(#2), and 5'-CACCGAAGACCAACTATGTTGTTT-3'(#3), respectively. Sequences were designed using the CRISPR DESIGN tool (http://crispr.mit.edu/). All specific target sequences were amplified and cloned,

and verified by DNA sequencing. After the transient transfection of pX330-sgParafibromin plasmids together with a puromycin-resistant plasmid into cells by using Lipofectamine reagent (Invitrogen), puromycin (2 μg/ml) (Invitrogen) treatment for 7 d was employed for selection and then cells were expanded in the regular culture medium.

Antibodies

Anti-FLAG (M2, SIGMA), anti-HA (3F10, Roche and 16B12, COVANCE), anti-YAP/TAZ (D24E4, Cell Signaling), anti-Parafibromin (A300-170A and A300-171A, Bethyl), anti-β-catenin (H102, Santa Cruz), anti-c-Myc (9E10, Santa Cruz), anti-Cyclin D1 (H295, Santa Cruz) and anti-Actin (C-11, Santa Cruz) antibodies were used as primary antibodies for immunoblotting.

Luciferase assay

Luciferase activities were measured by using the dual luciferase reporter assay (Promega) according to the manufacturer's protocol. pRL/TK-luciferase reporter plasmid was used as a second reporter. The data were obtained by analyzing triplicated samples. The pSP65-SRα, pcDNA3, pSUPER or pX330 empty vector was used for a control plasmid.

Immunoprecipitation and immunoblotting

Cells were harvested and lysed in lysis buffer containing 100 mM NaCl, 50 mM Tris-HCl (pH 8.0), 5 mM EDTA, 1% Brij35, 2 mM Na_3VO_4, 10 mM NaF, 2 mM β-glycerophosphate and 2 mM PMSF. For immunoprecipitation, lysates were incubated with respective antibodies and protein G-beads (GE Healthcare). The beads were then washed five times with the lysis buffer, and the immune complex was eluted with SDS–PAGE sample buffer. Lysates and immunoprecipitates were subjected to SDS-PAGE, followed by immunoblotting. Proteins were visualized using western blot chemiluminescence reagent (Perkin-Elmer Life Sciences). The obtained chemiluminescence was exposed to X-ray film (Fuji Film).

Immunostaining

AGS cells were washed with PBS and fixed with 4% paraformaldehyde. Cells were then permeabilized with 0.1% TritonX-100 and incubated in 1% BSA/PBS, followed by first antibody treatment. Fluorescent images were obtained using FV1200 (OLYMPUS) confocal microscope systems.

Quantitative RT-PCR

Quantitative RT-PCR was performed as previously described (Takahashi et al., 2011). Briefly, RNA extracted from cells using TRIzol reagent (Invitrogen) were subjected to reverse transcription by SuperScriptII (Invitrogen). cDNAs were analyzed by Step-One-Plus Real-Time PCR System (Applied Biosystems) using SYBR Premix Ex Taq (TaKaRa, Japan). *GAPDH* was used to normalize input. Following primers were used:

human *GAPDH*, 5'-CCTCAACTACATGGTTTACATGTTCC-3' and
5'-GAAGATGGTGATGGGATTTCCATTG-3';
mouse *Ctgf*, 5'-GGACACCTAAAATCGCCAAGC-3' and
5'-ACTTAGCCCTGTATGTCTTCACA-3';
mouse *Cyr61*, 5'-ATCTGCAGAGCTCAGTCAGAAGG-3' and
5'-AGACAGTTCTTGGGGACACAGAGG-3'.

Wound healing assay

Wound healing assay was performed as previously described (Tang et al., 2015). Briefly, AGS cells (4×10^5 cells) were cultured in six-well plate and were transfected with indicated expression vectors. 24 h after transfection, cells were subjected to serum starvation for 12 h. After rinsed with medium to remove unattached cells, the confluent layer of cells was scratched with a sterile tip to create an artificial wound. Cell migration to the wounded gap was then monitored by microscopy after 9 h and the distance between the edges of the wound was analyzed using ImageJ software.

Colony formation assay

Colony formation assay was performed as previously described (Tang et al., 2015). Briefly, NIH3T3 cells were transfected with indicated expression vectors. At 24 h after transfection, the cells were seeded in 6-well plates at a density of 1000 cells/well in 2 ml medium. After culturing for two weeks, colonies were stained with 0.5% crystal violet in 2% ethanol, and colonies were counted and photographed.

Cell proliferation assay

Cell proliferation assays were carried out in 96-well plates, and living cells were counted at each time point using MTS assays with a Cell Counting Kit (Promega) according to the manufacturer's instructions. Absorbance was measured at 450 nm.

Mice

Hrpt2$^{flox/flox}$ mice (Wang et al., 2008) were crossed with *CAG-CreER* transgenic mice to generate *Hrpt2*$^{flox/flox}$*;CAG-CreER* mice. At ages of 4 to 6 weeks, *Hrpt2*$^{flox/flox}$*;CAG-CreER* mice and the control littermates were daily injected intraperitoneally with tamoxifen dissolved in corn oil (4 mg/40 g body weight). Mice were euthanized and examined at 5 days after exposure to tamoxifen. All animals were treated and maintained in accordance with the protocol approved by the Ethics Committees for Animal Experiment at the Graduate School of Medicine, the University of Tokyo.

Immunohistochemistry

Freshly sampled mouse tissues were flushed with ice-cold PBS and fixed by incubation in 4% paraformaldehyde in PBS overnight at 4ºC. Fixed tissues were dehydrated, embedded in paraffin, and sectioned. The sections were de-waxed and rehydrated. Endogenous peroxidase activity was blocked by incubation in 0.3% hydrogen peroxide in methanol for 30 min at room temperature. Antigen retrieval was performed by boiling for 15 min in Citrate buffer pH 6.0 or Tris-EDTA pH 9.0. Tissues were incubated overnight at 4ºC with the following primary antibodies: anti-CTGF (ab6992, Abcam, 1:400), anti-CYR61 (ab24448, Abcam, 1:200) and anti-Parafibromin (A300-170A, Bethyl, 1:500). Staining was performed using the Vectastain ABC-Elite kit according to the manufacturer's instructions.

Statistics

All the numerous data were expressed as mean±SD, and were analyzed by two-tailed unpaired Student's t test. Statistical significance was assessed at $p<0.05$ and $p<0.01$. Representative experiments are shown.

Supplemental References

Tang, C., Mei, L., Pan, L.Y., Xiong, W.Y., Zhu, H.B., Ruan, H.F., Zou, C.C., Tang, L.F., Iguchi, T., and Wu, X.M. (2015). Hedgehog signaling through GLI1 and GLI2 is required for epithelial–mesenchymal transition in human trophoblasts. BBA-General Subjects 1850, 1438-1448.

Wang, P., Bowl, M.R., Bender, S., Peng, J., Farber, L., Chen, J., Ali, A., Zhang, Z., Alberts, A.S., Thakker, R.V., et al. (2008). Parafibromin, a component of the human PAF complex, regulates growth factors and is required for embryonic development and survival in adult mice. Mol. Cell. Biol. 28, 2930-2940.